

UNCLASSIFIED

| |
|---|
| |
| |
| |
| AD NUMBER |
| ADB042815 |
| NEW LIMITATION CHANGE |
| TO Approved for public release, distribution unlimited |
| FROM Distribution authorized to U.S. Gov't. agencies only; Test and Evaluation; JUN 1979. Other requests shall be referred to Air Force Flight Dynamics Laboratory, Attn: FBR, Wright-Patterson AFB, OH 45433. |
| AUTHORITY |
| AFWAL ltr, 14 May 1984 |

THIS PAGE IS UNCLASSIFIED

AD B 042815

DDC FILE COPY

AFFDL-TR-79-3087

LEVEL II

2

FORWARD SWEPT WING STATIC AEROELASTICITY

Terrence A. Weisshaar

Virginia Polytechnic Institute and State University
Aerospace and Ocean Engineering Department
Blacksburg, Virginia 24061

June 1979

FINAL REPORT FOR PERIOD JULY 1978 - APRIL 1979

Distribution limited to U.S. Government agencies only; test and evaluation; June 1979. Other requests for this document must be referred to the Air Force Flight Dynamics Laboratory (FBR), Wright-Patterson Air Force Base, Ohio 45433.

AIR FORCE FLIGHT DYNAMICS LABORATORY
AIR FORCE WRIGHT AERONAUTICAL LABORATORIES
AIR FORCE SYSTEMS COMMAND
WRIGHT-PATTERSON AIR FORCE BASE, OHIO 45433

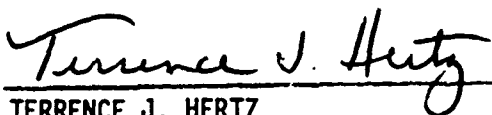
DDC
RECEIVED
DEC 26 1979
E

79 12 17 109

NOTICE

When Government drawings, specifications, or other data are used for any purpose other than in connection with a definitely related Government procurement operation, the United States Government thereby incurs no responsibility nor any obligation whatsoever, and the fact that the government may have formulated, furnished, or in any way supplied the said drawings, specifications, or other data, is not to be regarded by implication or otherwise as in any manner licensing the holder or any other person or corporation, or conveying any rights or permission to manufacture, use, or sell any patented invention that may in any way be related thereto.

This technical report has been reviewed and is approved for publication.




TERRENCE J. HERTZ
Project Engineer
Aeroelastic Group
Analysis and Optimization Branch



JAMES J. OLSEN, Acting Chief
Analysis and Optimization Br
Structures and Dynamics Division

FOR THE COMMANDER:



RALPH L. KUSTER, Col, USAF
Chief, Structures and Dynamics Division

"If your address has changed, if you wish to be removed from our mailing list, or if the addressee is no longer employed by your organization please notify AFFDL/FBR, W-P AFB, OH 45433 to help us maintain a current mailing list".

Copies of this report should not be returned unless return is required by security considerations, contractual obligations, or notice on a specific document.

SECURITY CLASSIFICATION OF THIS PAGE (When Data Entered)

| REPORT DOCUMENTATION PAGE | | READ INSTRUCTIONS BEFORE COMPLETING FORM |
|--|--|---|
| 1. REPORT NUMBER (18) AFFDL-TR-79-3487 | 2. GOVT ACCESSION NO. | 3. RECIPIENT'S CATALOG NUMBER |
| 4. TITLE (and Subtitle) (6) Forward Swept Wing Static Aeroelasticity | 5. TYPE OF REPORT & PERIOD COVERED (9) Final Report Jul 78 - Apr 79 | 6. PERFORMING ORG. REPORT NUMBER |
| 7. AUTHOR(s) (10) Terrence A. Weisshaar | 8. CONTRACT OR GRANT NUMBER(s) (15) AFOSR-77-3423 DARPA Order-3436 | 9. PROGRAM ELEMENT, PROJECT, TASK AREA & WORK UNIT NUMBERS PE: 62702E DARPA Order No. 3436 Task: 343600 |
| 10. PERFORMING ORGANIZATION NAME AND ADDRESS Virginia Polytechnic Institute & State University Aerospace & Ocean Engineering Department Blacksburg, Virginia 24061 | 11. CONTROLLING OFFICE NAME AND ADDRESS Air Force Flight Dynamics Laboratory (FBR) Air Force Wright Aeronautical Laboratories (AFSC) Wright-Patterson AFB, Ohio 45433 | 12. REPORT DATE (11) Jun 79 |
| 13. MONITORING AGENCY NAME & ADDRESS (if different from Controlling Office) (12) 58/ (16) 3436 (17) 80/ | 14. SECURITY CLASS. (of this report) Unclassified | 15. DECLASSIFICATION DOWNGRADING SCHEDULE |
| 16. DISTRIBUTION STATEMENT (of this Report) Distribution limited to U.S. Government agencies only; test and evaluation June 1979. Other requests for this document must be referred to the Air Force Flight Dynamics Laboratory (FBR), Wright-Patterson Air Force Base, Ohio 45433. | | |
| 17. DISTRIBUTION STATEMENT (of the abstract entered in Block 20, if different from Report) | | |
| 18. SUPPLEMENTARY NOTES | | |
| 19. KEY WORDS (Continue on reverse side if necessary and identify by block number) Aeroelastic Tailoring Composites Forward Swept Wings | | |
| 20. ABSTRACT (Continue on reverse side if necessary and identify by block number) In this report, laminated beam theory is used to predict the subcritical static aeroelastic behavior of swept wings constructed of laminated com- posite materials. Aerodynamic strip theory airloads are used to develop meaningful expressions for the flexible-to-rigid lift ratio and spanwise center of pressure movement of a swept wing as functions of wing aero- elastic parameters for a uniform property wing. A simple matrix method analysis approach to wing subcritical static aeroelastic response is detailed. | | |

DD FORM 1 JAN 73 1473 EDITION OF 1 NOV 65 IS OBSOLETE

SECURITY CLASSIFICATION OF THIS PAGE (When Data Entered)

406 922

FOREWORD

The information described in this report was authored by Virginia Polytechnic Institute and State University, Aerospace and Ocean Engineering Department, Blacksburg, Virginia, under AFOSR Grant 77-3423D, "Aeroelastic Stability and Performance Characteristics of Aircraft with Advanced Composite Sweptforward Wing Structures", and DARPA Order No. 3436. The work was administered by Mr. T. J. Hertz, Project Engineer, of the Structures and Dynamics Division (FBRC) of the Air Force Flight Dynamics Laboratory.

The contracted work was performed between July 1978 and April 1979. Dr. T. A. Weisshaar, Associate Professor of Aerospace and Ocean Engineering, Virginia Polytechnic Institute and State University (VPI&SU) was the principal investigator.

| | |
|---------------------|--|
| Accession For | |
| NTIS GRA&I | <input checked="checked" type="checkbox"/> |
| DDC TAB | <input type="checkbox"/> |
| Unannounced | <input type="checkbox"/> |
| Justification | |
| By _____ | |
| Distribution/ _____ | |
| Availability Codes | |
| Dist | Available/or special |
| B | |

TABLE OF CONTENTS

| SECTION | PAGE |
|--|------|
| I. INTRODUCTION | 1 |
| II. SUBCRITICAL STATIC AEROELASTIC RESPONSE- UNIFORM PLANFORM WING, STRIP THEORY AIRLIFTS | 4 |
| 1. Slender Composite Swept Wing Equilibrium Equations | 4 |
| 2. Aeroelastic Effect Equation Solution | 8 |
| 3. Discussion of Results | 10 |
| a. The Change in the Position of the Center of Pressure | 10 |
| b. Example Case | 13 |
| III. MODERATE TO HIGH-ASPECT-RATIO WING OF ARBITRARY PLANFORM IN SUBSONIC FLOW | 17 |
| 1. The Aeroelastic Equations in Matrix Form | 17 |
| 2. An Example Case | 24 |
| IV. Conclusions | 29 |
| APPENDIX A - The development of the Wing Flexibility Matrix | 30 |
| APPENDIX B - The Aerodynamic Influence Coefficient Matrix | 40 |
| APPENDIX C - Twist Caused by Control Deflection Pitching Moment | 43 |
| APPENDIX D - The Stiffness Expressions for a Laminated Composite Box Beam | 45 |
| REFERENCES | 50 |

LIST OF ILLUSTRATIONS

| FIGURE | PAGE |
|--------|---|
| 1 | Geometry of idealized swept wing, showing a chordwise section used in the computation of aerodynamic loads..... 5 |
| 2 | Static aeroelastic characteristics of a uniform property swept wing, showing spanwise center of pressure change Δy^* as a function of the parameters a and b/a 12 |
| 3 | A graph of a versus b/a for a uniform property wing at zero sweep with various fiber orientations θ shown. The dynamic pressure for this graph is the divergence dynamic pressure occurring when $\theta = 90^\circ$ 15 |
| 4 | A graph of a versus b/a for a uniform property wing at two sweep angles, $\Lambda = -15^\circ$ and $\Lambda = +15^\circ$. The dynamic pressure for this graph is the divergence dynamic pressure that occurs when $\theta = 90^\circ$ and $\Lambda = 0^\circ$ 16 |
| 5 | Wing aerodynamic model idealization; (a) actual planform, (b) planform idealization..... 18 |
| 6 | Nondimensional divergence velocity versus fiber orientation for a 30° forward swept wing. Sea level conditions, incompressible fluid. Wing taper ratio is 0.50..... 25 |
| 7 | The effect of fiber orientation on the spanwise position of the center of pressure of a wing with 30° of forward sweep. The dynamic pressure is $0.2 q_0$ of the wing when $\theta = 90^\circ$ 27 |
| 8 | Aileron effectiveness, for a wing with 30° of forward sweep, as a function of θ . Each curve is normalized with respect to the effectiveness of the ailerons on a rigid wing..... 28 |

LIST OF SYMBOLS

- a_0 = 2-dimensional lift curve slope of wing sections
- a = aeroelastic parameter, Equation 8
- b = aeroelastic parameter, Equation 9
- c = wing chord dimension measured in a direction perpendicular to the reference axis
- c_{mac} = aerodynamic pitching moment coefficient, measured perpendicular to the reference axis
- c_1^r = 2-dimensional lift coefficient for wing sections perpendicular to the reference axis of a rigid wing
- d = distance between line of centers of mass and reference axis, positive when the reference axis is aft
- e = distance between line of aerodynamic centers and reference axis, positive when the reference axis is aft
- f_1, f_2 = loading functions, Equations (10) and (11)
- g = K/GJ
- h = upward deflection of wing reference axis
- k = K/EI
- K = laminate coupling parameter, Appendix D
- l = length of swept wing span from root to tip, measured along the reference axis
- L = total lift generated by one wing
- M = bending moment about an axis perpendicular to the wing root
- n = load factor, equal to unity for 1-g flight
- p = upward load per unit length along the reference axis

LIST OF SYMBOLS (Continued)

| | |
|----------------|--|
| q | = dynamic pressure, $\frac{1}{2}\rho V^2$ |
| t | = nose-up torque per unit length along the reference axis |
| w | = wing weight per unit length along reference axis |
| y | = distance from wing root, measured along the reference axis |
| \bar{Y}_{CP} | = position of wing center of lift, measured along the reference axis |
| α | = nose-up rotation |

SECTION 1

INTRODUCTION

The recent interest in the application of laminated composite materials to forward swept wing structural design has led to studies indicating that static aeroelastic performance may be enhanced considerably by aeroelastic tailoring of forward swept wing structures. Reference 1 describes, in detail, the background of the forward swept wing concept and, in addition, presents an algebraic expression relating the divergence speed of swept wings to the geometric, aerodynamic and structural parameters of such wings. The present report describes the fundamental behavior of swept wings constructed with composites in the sub-critical flight regime.

The spanwise lift distribution acting upon a wing dictates the structural design of the wing support structure. Aeroelastic effects occur because the aerodynamic loads cause deformation of a flexible structure. These deformations cause changes in the shape of the lifting surface that, in turn, lead to changes in the applied loads. These interrelated effects occur until a deformed equilibrium state is reached for which the internal forces due to deformation balance the modified aerodynamic loads. The flexibility of a lifting surface, because of its effect on the magnitude and distribution of the external loads, causes changes in the wing lift-curve slope, wing bending and torsional moments, the spanwise center of pressure and, for swept wings, changes in the aircraft longitudinal center of pressure. Aeroelastic deformation and its effect upon spanwise loading is recognized to be important in a number of situations such as: wings operating at high dynamic pressures; thin wings; swept wings; and wings designed for low wing loading [2].

For a given wing, the effect of static aeroelasticity will increase with flight dynamic pressure since the lift per unit change in angle of attack is proportional to dynamic pressure. It is theoretically possible to encounter a flight condition for which the change in the external lift load due to structural deformation exceeds the structural restoring forces within the structure. This condition produces the structural instability referred to as wing aeroelastic divergence.

Modern day computerized computational methods now exist to analyze the effects of static aeroelasticity upon modern composite wings. However, since these methods require a reasonable amount of knowledge of the structural characteristics of the wing itself, they are fairly cumbersome and inefficient to use for parameter studies whose intent is to develop information about the qualitative behavior of laminated composite structures. A need exists to determine some of the more important consequences and benefits of the use of aeroelastic tailoring on swept wing structures.

The present study extends the studies presented in Reference 1 to discuss the potential for utilization of laminated composite materials to enhance the pre-divergence or sub-critical static aeroelastic characteristics of swept wings in general and forward swept wings in particular. Specifically to be considered in the present report are: the effects of laminate parameters such as fiber orientation and laminate lay-up on divergence; load redistribution; and lateral control effectiveness of swept wings.

To accomplish these objectives, two theoretical models were formulated for the present study. The first of these models uses a laminated box-beam idealization, together with simple strip theory air loads, to study

the spanwise lift redistribution problem that arises for flexible, uniform planform, swept wings. The other model uses a more general laminated box-beam idealization of the wing structure, and employs a more accurate and versatile representation of the aerodynamic loading to study more realistic configurations.

SECTION II

SUBCRITICAL STATIC AEROELASTIC RESPONSE - UNIFORM PLANFORM WING, STRIP THEORY AIRLOADS

The differential equations of equilibrium for a slender wing with moderate-to-high aspect-ratio may be formulated easily when the spanwise centerline of the wing box is restricted to be a straight line and the deformations of the wing are described in terms of elementary Euler-Bernoulli beam bending theory. This approach is used by Diederich and Foss [2] to study the static aeroelastic behavior of metallic swept wings. In this section this elementary approach is used to study the static aeroelastic deformation problem for composite swept wings. The resulting equations are solved for the simple case in which the geometrical and structural properties are constant along the wing span.

1. SLENDER COMPOSITE SWEPT WING EQUILIBRIUM EQUATIONS

The differential equations of equilibrium, in terms of bending and torsional deformations, of a slender swept wing may be formulated by considering the aerodynamic loads to act upon chordwise segments of the wing, perpendicular to the wing reference axis, as shown in Figure 1. The structural model for the wing assumes the loads to be carried by a box beam arrangement constructed of laminated composite materials forming the upper and lower face-sheets of the wing box. The reference axis, labelled as the y axis in Figure 1, is located equidistant between the front and rear edges of the box beam and lies in the geometric midplane of the box, halfway between the upper and lower surfaces of the cover sheets.

Reference 1 describes, in detail, the theoretical development of the laminated-composite, box-beam, structural model. The governing equations

of equilibrium for such a wing are found to be (note that $()' = d()/dy$ in what follows):

$$(EIh'' - K\alpha')' = p(y) \quad (1)$$

$$(-Kh'' + GJ\alpha')' = -t(y) \quad (2)$$

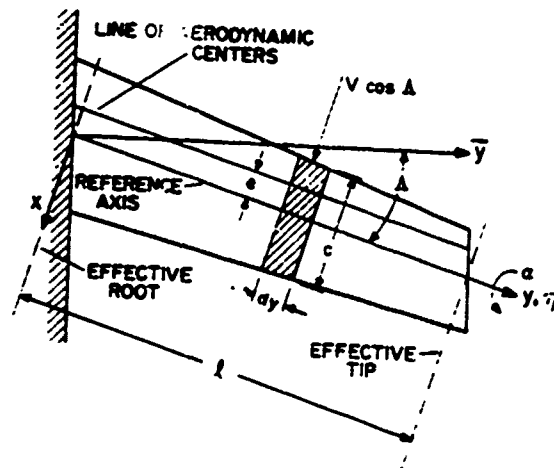


Figure 1 - Geometry of idealized swept wing, showing a chordwise section used in the computation of aerodynamic loads.

The structural parameters EI , GJ and K are the beam bending stiffness, torsional stiffness and bending-torsion coupling parameter, respectively, and are derived and defined in Reference 1. These quantities are given in Appendix D. The variables $h(y)$ and $\alpha(y)$ represent the upward bending displacement of the wing reference axis and the nose-up twisting rotation of the wing sections, respectively. The term $p(y)$ is the upward load per unit length, measured along the y -axis, while $t(y)$ is the nose-up torque per unit length, also measured along the y -axis.

Reference 3 describes one method that may be used to compute the wing loads $p(y)$ and $t(y)$ for this type of slender wing model. For this

calculation, aerodynamic strip theory is used to develop the following expressions:

$$p(y) = cc_{\ell}^r q \cos^2 \Lambda + qca_0 \cos^2 \Lambda (\alpha - r \tan \Lambda) - nw \quad (3)$$

$$t(y) = qcec_{\ell}^r \cos^2 \Lambda + qc^2_{c_{mac}} \cos^2 \Lambda - nwd \\ + qcea_0 (\alpha - r \tan \Lambda) \cos^2 \Lambda \quad (4)$$

In equations (3) and (4), the term c_{ℓ}^r corresponds to the two-dimensional lift coefficient for wing sections perpendicular to the reference axis for a wing with no flexibility, while a_0 refers to the two-dimensional lift-curve slope of the same section. r is the slope of the bending deformation, defined as $r = dh/dy$, while nw represents the distributed inertia load per unit length for a wing of weight w pounds per unit length operating at a load factor n . The substitution of Equation (3) into Equation (1), and Equation (4) into Equation (2) provides the differential equations of equilibrium that govern the static aeroelastic response problem. Equation (1) is the bending equation and can be nondimensionalized to yield the following relationship:

$$\frac{d^3 \Gamma}{d\eta^3} - k \frac{d^3 \alpha}{d\eta^3} + \frac{qc\ell^3 a_0 \cos^2 \Lambda}{EI} (\alpha - r \tan \Lambda) \\ = -qc\ell^3 c_{\ell}^r \cos^2 \Lambda / EI + nw\ell^3 / EI \quad (5)$$

where $\eta = i - y/l$ and $r = \frac{dh}{dy}$.

With similar nondimensional definitions, Equation (2), the torsion equation, becomes:

$$\begin{aligned} \frac{d^2 g}{d\eta^2} - g \frac{d^2 r}{d\eta^2} + \frac{qce_l^2 a_0 \cos^2 \Lambda}{GJ} (\alpha - r \tan \Lambda) \\ = \frac{-qce_l^2 c_l^r \cos^2 \Lambda}{GJ} \left(1 + \left(\frac{c}{e} \right) \left(\frac{c_{mac}}{c_l^r} \right) \right) + nwd_l^2 / GJ \end{aligned} \quad (6)$$

Equations (5) and (6) are coupled together by the dependence of the aerodynamic load upon the term $(\alpha - r \tan \Lambda)$ and by the structural coupling parameter K and its nondimensional counterparts $k = K/EI$ and $g = K/GJ$. These two equations can be combined to form a single equation in terms of a new variable α_e , defined as $\alpha_e = \alpha - r \tan \Lambda$. The procedure used to achieve this combination is as follows:

- 1) Differentiate the torsion equation, Equation (6) with respect to η ; then, multiply the result by the factor $(1 - k \tan \Lambda)$.
- 2) Multiply the bending equation, Equation (5), by the factor $(g - \tan \Lambda)$.
- 3) Add the two above results together to obtain the following equation;

$$\alpha_e''' + a\alpha_e' - b\alpha_e = f_1' - f_2 \quad (7)$$

with the definitions of terms a, b, f_1, f_2 given as

$$a = \left(\frac{qce_l^2 a_0 \cos^2 \Lambda}{GJ} \right) \left(\frac{1 - k \tan \Lambda}{1 - kg} \right) \quad (8)$$

$$b = \left(\frac{qce_l^3 a_0 \cos^2 \Lambda}{EI} \right) \left(\frac{\tan \Lambda - g}{1 - kg} \right) \quad (9)$$

$$f_1 = \left(\frac{1 - k \tan \Lambda}{1 - kg} \right) \left[- \left(1 + \left(\frac{c}{e} \right) \left(\frac{c_{mac}}{c_l^r} \right) \left(\frac{q c e l^2 c_l^r \cos^2 \Lambda}{GJ} \right) + \frac{n w d l^2}{GJ} \right) \right] \quad (10)$$

$$f_2 = \left(\frac{g - \tan \Lambda}{1 - kg} \right) \left[\frac{q c l^3 c_l^r \cos^2 \Lambda}{EI} - \frac{n w l^3}{EI} \right] \quad (11)$$

The boundary conditions, in terms of the variable α_e , are found by first noting that both r (the bending slope) and α are zero at the effective root of the wing ($\eta = 1$). This leads to the boundary condition

$$\alpha_e(\eta = 1) = 0 \quad (12)$$

The fact that the bending moment and the twist are zero at the effective wing tip leads to the equation

$$\alpha_e'(\eta = 0) = 0 \quad (13)$$

The wing tip zero shear condition, when combined with the torsion equation, evaluated at $\eta = 0$, leads to the following result:

$$\alpha_e''(0) + a \alpha_e(0) = f_1(0) \quad (14)$$

2. AEROELASTIC EFFECT EQUATION SOLUTION

To solve the wing deformation problem defined by Equation (7) and its associated boundary conditions, we restrict ourselves to an untwisted, uniform planform wing whose pitch attitude is specified. In this case, $f_1(\eta)$ and $f_2(\eta)$ are constants. It is shown in References 2 and 3 that the solution to this problem is given by

$$\alpha_e(\eta) = \frac{f_2}{b} \left[1 - \frac{f_3(\eta)}{f_3(1)} \right] \quad (15)$$

The function $f_3(\eta)$ is defined as

$$f_3(\eta) = \left[\frac{4\beta^2}{9\beta^2 + \gamma^2} \right] e^{-2\beta\eta} + e^{\beta\eta} \left[\left(\frac{5\beta^2 + \gamma^2}{9\beta^2 + \gamma^2} \right) \cos\gamma\eta + \left(\frac{3\beta^3 - \beta\gamma^2}{9\beta^2\gamma + \gamma^3} \right) \sin\gamma\eta \right] \quad (16)$$

The terms β and γ that appear in Equation (16) are obtained from the knowledge that -2β and $\beta \pm i\gamma$ are roots of the following characteristic equation, obtained from Equation (7),

$$r^3 + ar - b = 0 \quad (17)$$

If the parameters c_1 and c_2 are defined as

$$c_1 = \left[\frac{b}{2} + \sqrt{\frac{b^2}{4} + \frac{a^3}{27}} \right]^{1/3} \quad (18)$$

$$c_2 = \left[\frac{b}{2} - \sqrt{\frac{b^2}{4} + \frac{a^3}{27}} \right]^{1/3} \quad (19)$$

then β and γ may be written as

$$\beta = -\frac{1}{2} (c_1 + c_2) \quad (20)$$

$$\gamma = \frac{\sqrt{3}}{2} (c_1 - c_2) \quad (21)$$

Equation (15) provides information necessary to compute the ratio between the total lift developed by a flexible composite wing and the lift developed by a similar, but inflexible wing. Under the strip theory restriction, the lift of the rigid wing is found to be

$$L_r = qcc_l^r \ell \cos^2\Lambda - n\omega\ell \quad (22)$$

The lift on the flexible wing is

$$L = L_r + \int_0^\ell (qc a_0 \cos^2\Lambda) \alpha_e dy \quad (23)$$

Performing the necessary integration in Equation (23) and dividing by L_r yields an expression for the flexible-to-rigid wing lift ratio:

$$\frac{L}{L_r} = \frac{-2\beta\gamma e^{-2\beta} + 2\beta\gamma e^{\beta} \cos\gamma + (3\beta^2 + \gamma^2)e^{\beta} \sin\gamma}{4\beta^2 e^{-2\beta} + e^{\beta}[(5\beta^2 + \gamma^2) \cos\gamma + (3\beta^2 - \beta\gamma^2) \sin\gamma]} \quad (24)$$

Equation (24) is an expression for the lift effectiveness of the wing. Note that when the denominator becomes zero, then the wing will diverge.

The ratio of the bending moment at the wing root for the flexible wing to that computed for the rigid wing is found to be

$$\frac{M}{M_r} = 2 \left[\frac{\gamma e^{-2\beta} + e^{\beta}(-\gamma \cos\gamma + 3\beta \sin\gamma)}{4\beta^2 \gamma e^{-2\beta} + e^{\beta}[(5\beta^2 \gamma + \gamma^3) \cos\gamma + (3\beta^3 - \beta\gamma^2) \sin\gamma]} \right] \quad (25)$$

The bending moment is measured about the effective root of the wing as shown in Figure 1.

The twisting moment ratio expression is identical to that calculated for the ratio L/L_r . The spanwise center of pressure, Y_{CP} , measured along the reference axis, can be obtained by combining Equations (24) and (25) and reads as follows:

$$Y_{CP} = \frac{\ell}{2} \left(\frac{M}{M_r} \right) \left(\frac{L_r}{L} \right) \quad (26)$$

3. DISCUSSION OF RESULTS

a. The Change in the Position of the Center of Pressure

The change in the spanwise position of the center of pressure, due to wing flexibility, affects both the overall directional stability of the aircraft and the wing root stresses. An outboard shift of the center of pressure results in an increase in stress levels near the wing root. The equations obtained previously may be used to compute the change in the spanwise location of the center of pressure position along the swept reference axis. Reference 2 presents a study of this change for uniform

planform metallic wings, as a function of two parameters. These parameters are related to dynamic pressure and to the sweep angle. The present study presents similar results by suitably redefining parameters to conform to the composite wing analysis. The two parameters are the parameter a , defined in Equation (8), and the ratio of b/a defined as follows:

$$\frac{b}{a} = \left(\frac{\ell}{e} \right) \left[\frac{\tan \Lambda - g}{1 - k \tan \Lambda} \right] \left[\frac{GJ}{EI} \right] \quad (27)$$

The parameter a is referred to as the dynamic pressure parameter, while b/a is termed the sweep parameter. Figure 2 shows the influence of these parameters upon the movement of the center of pressure (CP) along the swept reference axis. The parameter Δy^* is equal to $\Delta y_{CP}/\ell/2$, and positive Δy^* corresponds to an outward CP movement while, conversely, inboard CP movement is denoted by negative values of Δy^* .

Labelling the upper right quadrant of Figure 2 as Quadrant 1, and numbering the other quadrants consecutively, counterclockwise, we see that values of a and b/a that lie in Quadrant 1 correspond to wings for which divergence is very unlikely to occur. In addition, the center of pressure movement is inboard for values of b/a greater than about 4.

In Quadrant 2, divergence is very likely, except for wings falling into a very narrow range of a and b/a values. In addition, shifts in the CP location are outboard so that unfavorable effects of aeroelasticity upon wing stresses may be expected in this region.

In Quadrant 3, divergence is impossible, while, in Quadrant 4, divergence may be possible for certain combinations of a and b/a .

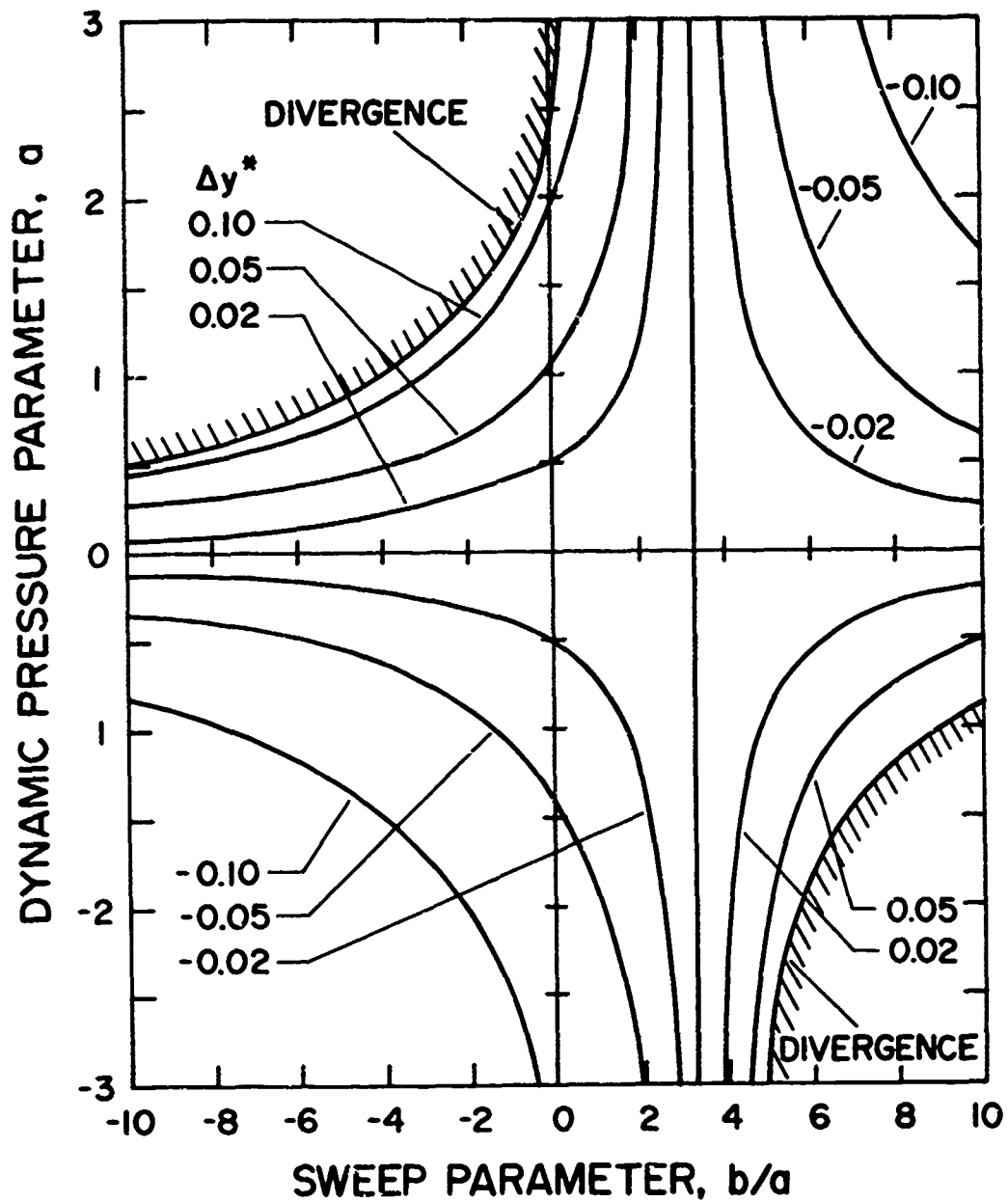


Figure 2- Static aeroelastic characteristics of a uniform property swept wing, showing spanwise center of pressure change Δy^* as a function of the parameters a and b/a

Reference 2 notes that subsonic, metallic sweptback wings ($k = g = 0$) are described by values of a and b/a lying in the first quadrant, while subsonic, metallic sweptforward wings fall into Quadrant 2. For a to be negative for a metallic wing, the chordwise aerodynamic center must lie behind the wing elastic axis. This situation is usually associated with supersonic flight. Quadrant 3 illustrates sweptforward metallic wing behavior in the supersonic flight regime, while Quadrant 4 displays metallic sweptback wing behavior at supersonic speeds.

When the wing is constructed of composite materials, the likely effect of sweep on aeroelastic behavior is not as clear as it is for metallic wings. The elastic coupling between bending and torsion introduces a new parameter into the definitions of a and b/a . For a particular value of wing sweep angle and dynamic pressure, the values of a and b/a may be modified by tailoring of the composite laminate.

b. Example Case

Figures 3 and 4 are presented to illustrate the potential effect of tailoring laminate fibers for aeroelastic performance. Consider first Figure 3, in which the parameter a is plotted versus the sweep parameter b/a for an example wing with zero sweep. The wing is one of constant chord and uniform elastic properties along the span. The laminated wing structure itself has a laminate thickness-to-box beam depth ratio of 1:10. The laminate cover sheets are composed of graphite-epoxy with 10% of the laminate fibers oriented along the x -axis (see Figure 1); 25% of the fibers are along the $\pm 45^\circ$ direction (with respect to the y -axis) and 65% of the fibers are oriented at a variable angle θ , measured with respect to the x -axis.

The dynamic pressure value chosen corresponds to q equal to the divergence q of an unswept wing with a laminate for which $\theta = 90^\circ$. The plot of a versus b/a is symmetrical about the vertical axis and exhibits a cusp. At this point, laminates with $\theta = 0^\circ$ and $\theta = 90^\circ$ exhibit the same static aeroelastic behavior. Referring back to Figure 2, it is seen that the effect of sweeping the θ fibers forward is to keep the wing static aeroelastic characteristics in Quadrant 1. The favorable performance of the wing structure in this region is readily apparent.

Figure 4 shows a plot of a versus b/a for two uniform property wings, one with 15° of forward sweep and the other with 15° of rearward sweep. The two plots are seen to be symmetrical about the line b/a equal to zero. For the $\Lambda = -15^\circ$ wing, a cusp point is located to the left of the origin and coincides with a wing with θ fibers at 0° and approximately 73° . The $\Lambda = +15^\circ$ wing has a similar cusp when $\theta = 0^\circ$ and $\theta = 107^\circ$. For this wing, it is still possible to design the laminate such that divergence will not occur, even for 15° of forward sweep. Sweeping the wing beyond 15° of forward sweep is found to move the cusp further to the left and to further distort the figure.

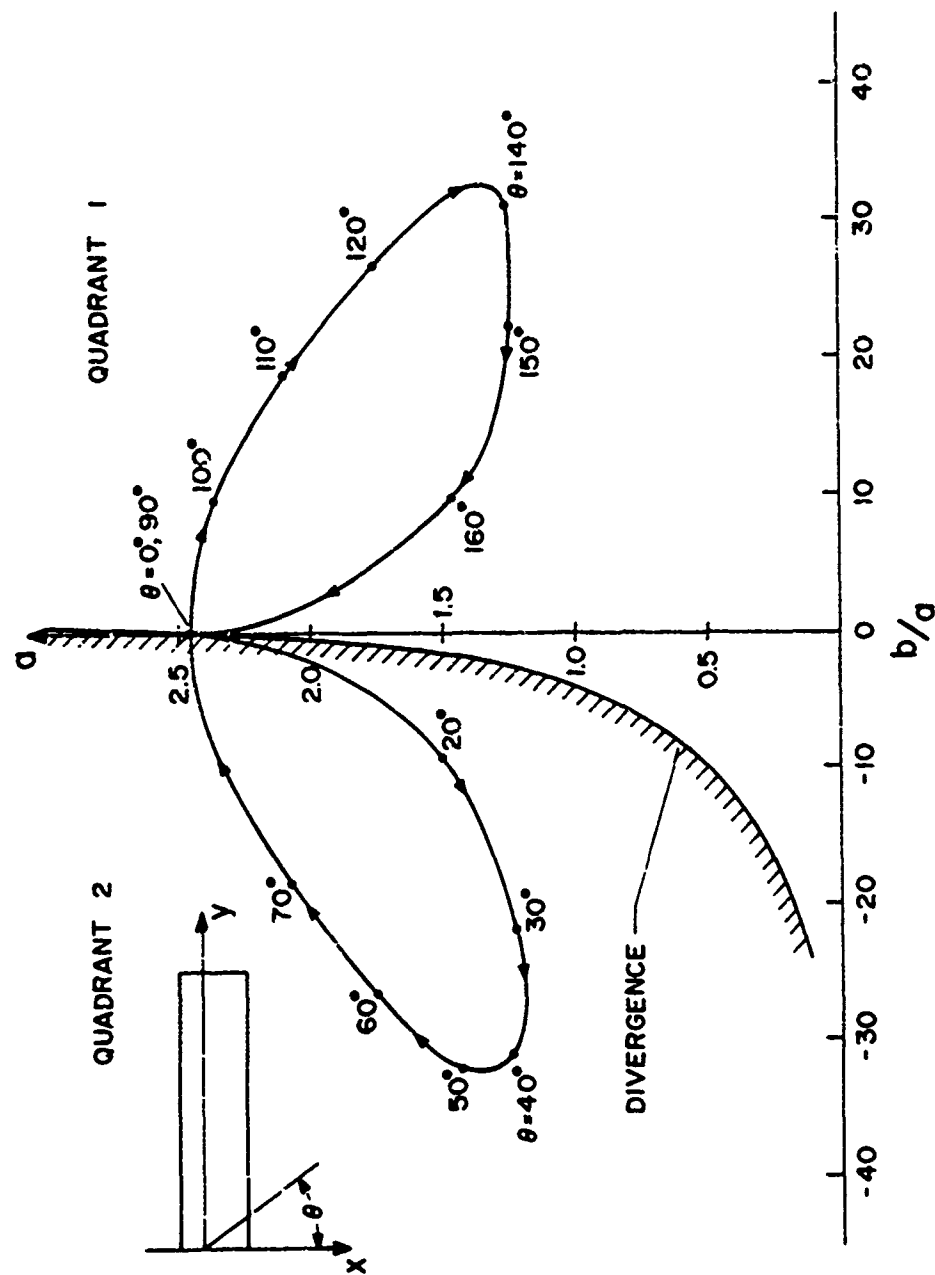


Figure 3- A graph of d versus b/a for a uniform property wing at zero sweep with various fiber orientations θ shown. The dynamic pressure for this graph is the divergence dynamic pressure occurring when $\theta = 90^\circ$.

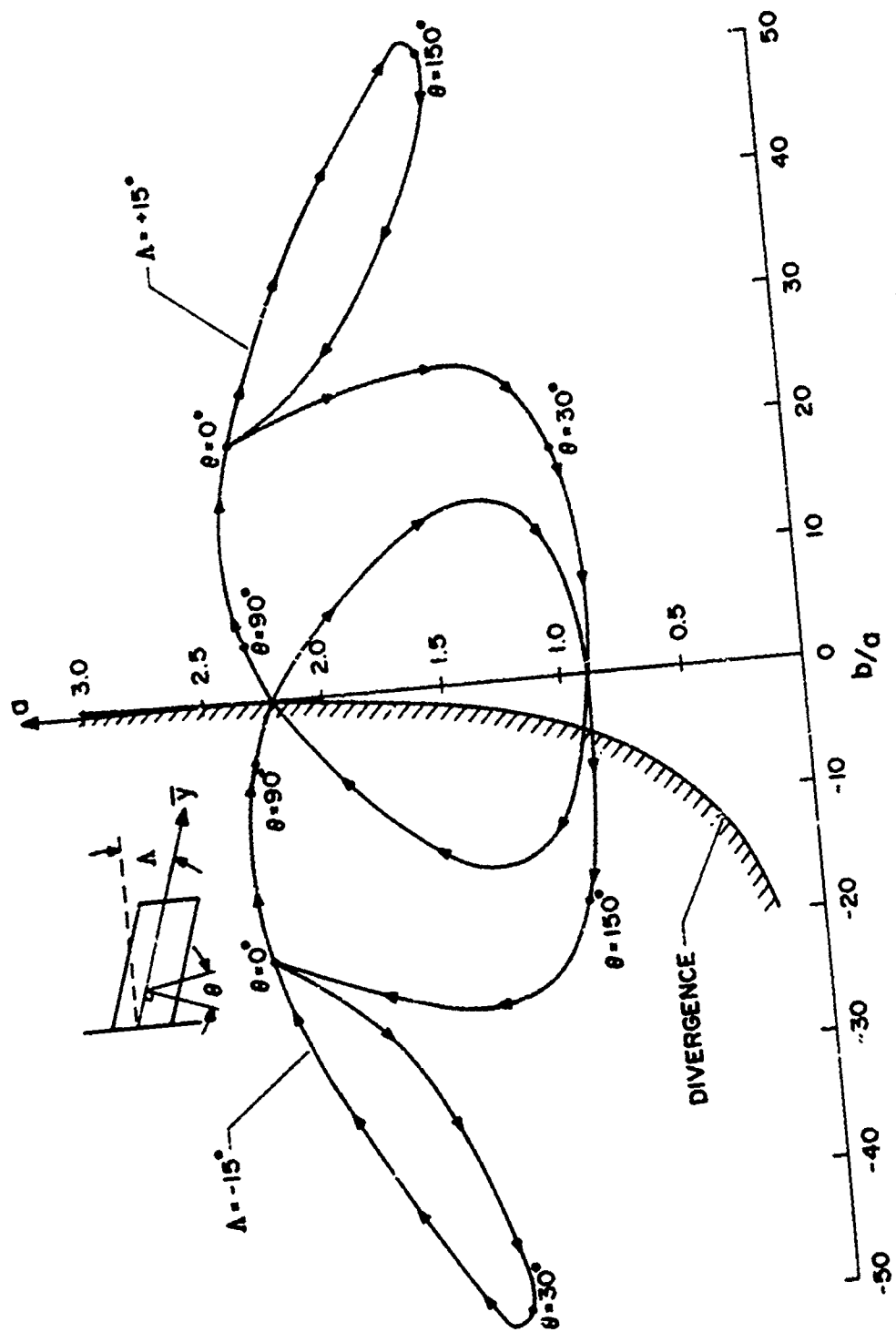


Figure 4- A graph of C_p versus b/a for a uniform property wing at two sweep angles, $\lambda = -15^\circ$ and $\lambda = +15^\circ$. The dynamic pressure for this graph is the divergence dynamic pressure that occurs when $\theta = 90^\circ$ and $\lambda = 0^\circ$.

SECTION III

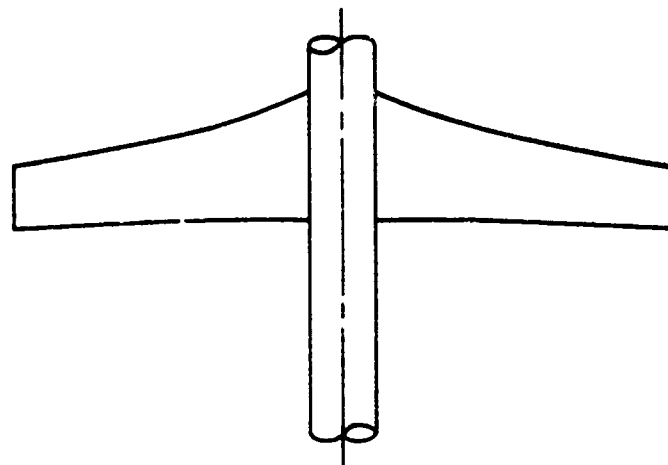
MODERATE TO HIGH-ASPECT-RATIO WING OF ARBITRARY PLANFORM IN SUBSONIC FLOW

This section discusses a computation method to determine the subcritical static deformation of a flexible, moderate-to-high-aspect-ratio wing in a subsonic flow. The wing planform itself may have an arbitrary shape, while the structural model is idealized to be a nonuniform box beam constructed of composite material. The wing aerodynamic forces are computed by use of a modified Weissinger L-method, valid at subcritical Mach numbers. The basic computational scheme is based upon that found in NACA TN 3030 [4], with the exception that the method has been updated to include composite material coupling effects such as those discussed previously in Section II of this report.

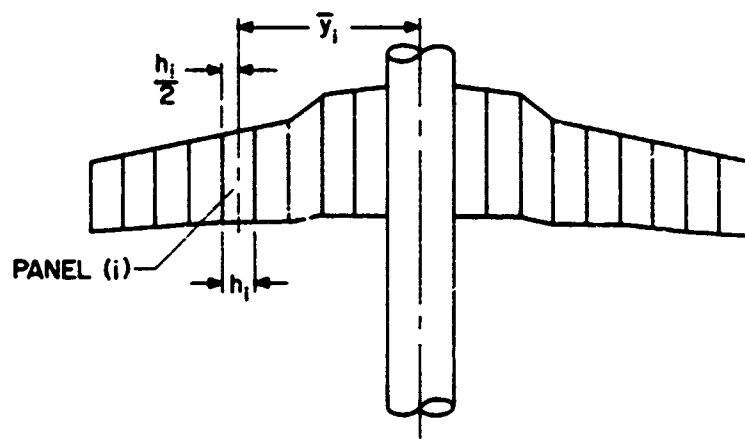
1. THE AEROELASTIC EQUATIONS IN MATRIX FORM

The subcritical static aeroelastic analysis problem can be reduced to finding the solution to a set of simultaneous linear algebraic equations. The first step in such an analysis is the formulation of a relationship between the airload distribution along the wing (lift per unit length) and the streamwise angle of attack distribution. The formulation of the problem involves the idealization of the continuous wing into a finite number of discrete panels. Figure 5 illustrates a typical wing idealization. The lift per unit length p_i is computed at the center-span of the panels, while the streamwise angle of attack α_i (positive nose-up) is measured at the same points. The lift acting on each panel is then equal to $p_i h_i$.

Denoting the lift intensity at a finite number of positions or panels



(a) ACTUAL PLAN FORM



(b) IDEALIZATION

Figure 5- Wing aerodynamic model idealization;
(a) actual planform, (b) planform
idealization

along the wing as a vector $\{p_i\}$ and the streamwise angle of attack distribution at the same positions as $\{\alpha_i\}$, a linear relationship can be written to relate $\{p_i\}$, $\{\alpha_i\}$ and the dynamic pressure, q . Expressed in standard matrix notation, this equation is

$$1/q[A_{ij}]\{p_j\} = \{\alpha_i\} \quad (28)$$

The square matrix $[A_{ij}]$ is the matrix of aerodynamic influence coefficients; the computation of this matrix is discussed in Appendix B. The distribution of angle of attack $\{\alpha_i\}$ along the wing is composed of three types of components, and is expressed as follows:

$$\{\alpha_i\} = \{\alpha_r\} + \{\alpha_s\} + \{\alpha_c\} \quad (29)$$

The portion of $\{\alpha\}$ denoted as $\{\alpha_r\}$ is a rigid body angle of attack and occurs either because of the incidence angle of the entire aircraft or because of a predetermined initial or "built-in" geometric angle of attack distribution along the wing. The vector $\{\alpha_s\}$ represents the angle of attack distribution caused by the deformation of the flexible wing structure.

The $\{\alpha_c\}$ distribution represents that part of the angle of attack distribution due to apparent or actual aerodynamic twists, such as those caused by aileron deflection or steady-state angular velocity due to aircraft roll motion.

The angle of attack distribution due to structural deformation is computed from the equation

$$\{\alpha_s\} = [C_{ij}]\{p_j\} \quad (30)$$

where C_{ij} represents an element of the wing flexibility matrix. For the computation of this matrix it is assumed that the wing semi-span is clamped at its root and free at the tip. The details of the formulation of

this matrix for a wing with a composite material wing box, idealized as a beam, are discussed in detail in Appendix A. These coefficients had not been derived previously in the open literature.

By combining Equations (28), (29) and (30), a basic relationship, relating loads to angles of attack, is found to be as follows:

$$[B_{ij}]\{p_j\} = \{\alpha_r\} + \{\alpha_c\} \quad (31)$$

where

$$[B_{ij}] = [1/q[A_{ij}] - [C_{ij}]] \quad (32)$$

Computational efficiency is achieved when the general wing airload distribution is subdivided into two basic types: those loads due to maneuvers resulting in symmetrical lift distributions; and those maneuvers, such as may result from aileron actuation, resulting in asymmetrical lift distribution. When this subdivision of load sets is used, only one wing semi-span need be studied. In Reference 4, and in this report, the left wing is used. Thus, the matrix $[B_{ij}]$ is computed for half the wing span, once for the symmetrical maneuver (e.g., the 1-g load) and once for the asymmetrical maneuver (e.g., the aileron effectiveness problem).

The matrix $[B_{ij}]$, as defined in Equation (32), is a function of the flight dynamic pressure, q . The solution for the airload distribution $\{p_i\}$ requires computation of the inverse of $[B_{ij}]$. Wing configurations, for which $[B_{ij}]$ is singular at certain critical values of q may exist. These critical values of q , denoted as q_D , correspond to the clamped wing static divergence dynamic pressures. For a symmetrical maneuver, the load distribution along the wing, is given by the expression

$$\{p_i\} = [B_{ij}]^{-1}\{\alpha_r\} \quad (33)$$

The total lift, L , of the wing is

$$L = 2 [1] \{p_i\} = 2 [1] [B_{ij}]^{-1} \{\alpha_r\} \quad (34)$$

If $\{\alpha_r\}$ is given by the equation

$$\{\alpha_r\} = \alpha_0 \{1\} \quad (35)$$

then Equation (34) is written as

$$L = 2 \alpha_0 [1] [B_{ij}]^{-1} \{1\} \quad (36)$$

The lift curve slope of the wing is written as

$$C_{L_\alpha} = L / (q S \alpha_0) \quad (37)$$

or

$$C_{L_\alpha} = (2/qS) [1] [B_{ij}]^{-1} \{1\} \quad (38)$$

where S is defined to be the total wing planform area. A two-dimensional sectional lift-curve slope is included in the input parameters that must be known before the A_{ij} coefficients can be calculated. The effect of Mach number on the wing lift-curve slope may be accounted for by modification of the 2-D sectional lift curve slopes for each section. The reader is referred to Reference 4 for a complete discussion of this modification.

The effectiveness of aileron deflection in generating roll may be computed by a method similar to that outlined for the symmetrical airload computation. Since ailerons are deflected asymmetrically to initiate and sustain rolling motion, the lift distribution that results from roll is asymmetrical. The asymmetrical influence of one wing semi-span upon the other is accounted for by proper computation of the aerodynamic influence coefficients. This matrix of coefficients for the asymmetrical lift case is denoted as $[A_{ij}^{(a)}]$.

The equation of equilibrium for an aircraft undergoing a steady-state roll may be written as:

$$\frac{1}{q} [A_{ij}^{(a)}] \{p_j\} = [C_{ij}] \{p_j\} + q[E_{ij}] \{\delta\} + \left\{ \frac{\partial \alpha}{\partial \delta} \right\} \delta + \frac{Pb}{2V} \left\{ \frac{2\bar{y}_i}{b} \right\} \quad (39)$$

Referring to the right-hand side of Equation (39), the first term corresponds to the angle of attack distribution due to structural flexibility. The second term, involving the square matrix $[E_{ij}]$, appears because the deflection of an aileron causes a change in the pitching moment of the various wing sections. This change in pitching moment produces a change in the angle of attack due to structural deformation and is proportional to q . The detailed development of the $[E_{ij}]$ matrix is discussed in Appendix C.

The third term in Equation (39) accounts for the apparent change in angle of attack of a wing section that occurs with aileron deflection. Finally, the term proportional to $Pb/2V$ represents the damping-in-roll term. This latter term appears because rolling motion of the wing (positive if the left wing moves down) produces an apparent change in angle of attack $\Delta\alpha_i$ at a position \bar{y}_i on the left wing, given by

$$\Delta\alpha_i = P\bar{y}_i/V \quad (40)$$

When the aircraft is in a steady-state roll condition, the equation for moment equilibrium becomes:

$$[\bar{y}_i] \{ p_i h_i \} = 0 \quad (41)$$

Equation (41) is used to solve for the amount of roll rate caused by an aileron deflection $\{\delta_i\}$ along the left wing, with a corresponding deflection $\{-\delta_i\}$ along the right wing.

Let $[B_{ij}^{(a)}] = [A_{ij}^{(a)}] - [C_{ij}]$ (42)

while $\{\delta_i\} = \delta_0 \{\psi\}$ (43)

Equation (43) allows segmented ailerons, although, in the usual case, this vector would be composed of values of 0 and -1, corresponding to no aileron or an "up aileron", respectively, at a wing station.

Using the definitions in Equations (41), (42) and (43), the following relationship is found

$$(Pb/2V)/\delta_0 = \frac{-[\bar{y}_i h_i][B_{ij}^{(a)}]^{-1} \{q[E_{ij}]\{\psi\} + \{\frac{\partial \alpha}{\partial \delta} \psi_i\}\}}{[\bar{y}_i h_i][B_{ij}^{(a)}]^{-1} \{\frac{2\bar{y}_i}{b}\}} \quad (44)$$

The quantity $(Pb/2V)/\delta_0$ is termed the aileron effectiveness. The aileron effectiveness is a measure of the effectiveness of lateral control devices and represents the wing-tip helix angle per radian of asymmetrical aileron displacement. When the aileron effectiveness is a positive quantity, positive roll control is possible. Since aileron effectiveness is a function of q , there may be situations for which q is large enough to cause control reversal, that is, the aileron effectiveness may be negative. The aileron reversal speed corresponds to the speed at which the aileron effectiveness is zero.

2. AN EXAMPLE CASE

To illustrate the use of the computational method described in the previous section, an example wing was developed. The wing planform has a linear taper and a tip-to-root chord ratio of 0.50; the reference axis is swept forward 30°. The chordwise sections of the wing are geometrically similar; this leads to a situation in which the bending stiffness, torsional stiffness and coupling parameter vary along the reference axis as follows.

$$EI = f^4 EI_r; GJ = f^4 GJ_r; K = f^4 K_r \quad (45)$$

where $f = 1 - n(1-\lambda)$

$$n = y/l$$

$$\lambda = \text{taper ratio} = c_{\text{tip}}/c_{\text{root}}$$

and

$$()_r = \text{wing root value}$$

The wing structure itself consists of thin, laminated cover sheets, top and bottom. These laminates are composed of graphite-epoxy lamina and have a layup identical to those described for the example in Section 2.3(b). The wing planform has a reference chord of 45 inches and a semi-span, $b/2$, of 120 inches.

Figure 6 shows a plot of nondimensional divergence velocity at sea level in incompressible flow. The reference velocity, V_R , corresponds to the divergence speed of the wing when the variable, or θ , fibers lie along the reference axis, $\theta = 90^\circ$. The maximum divergence velocity is seen to occur when θ is approximately 110° , or 20° forward of the reference axis.

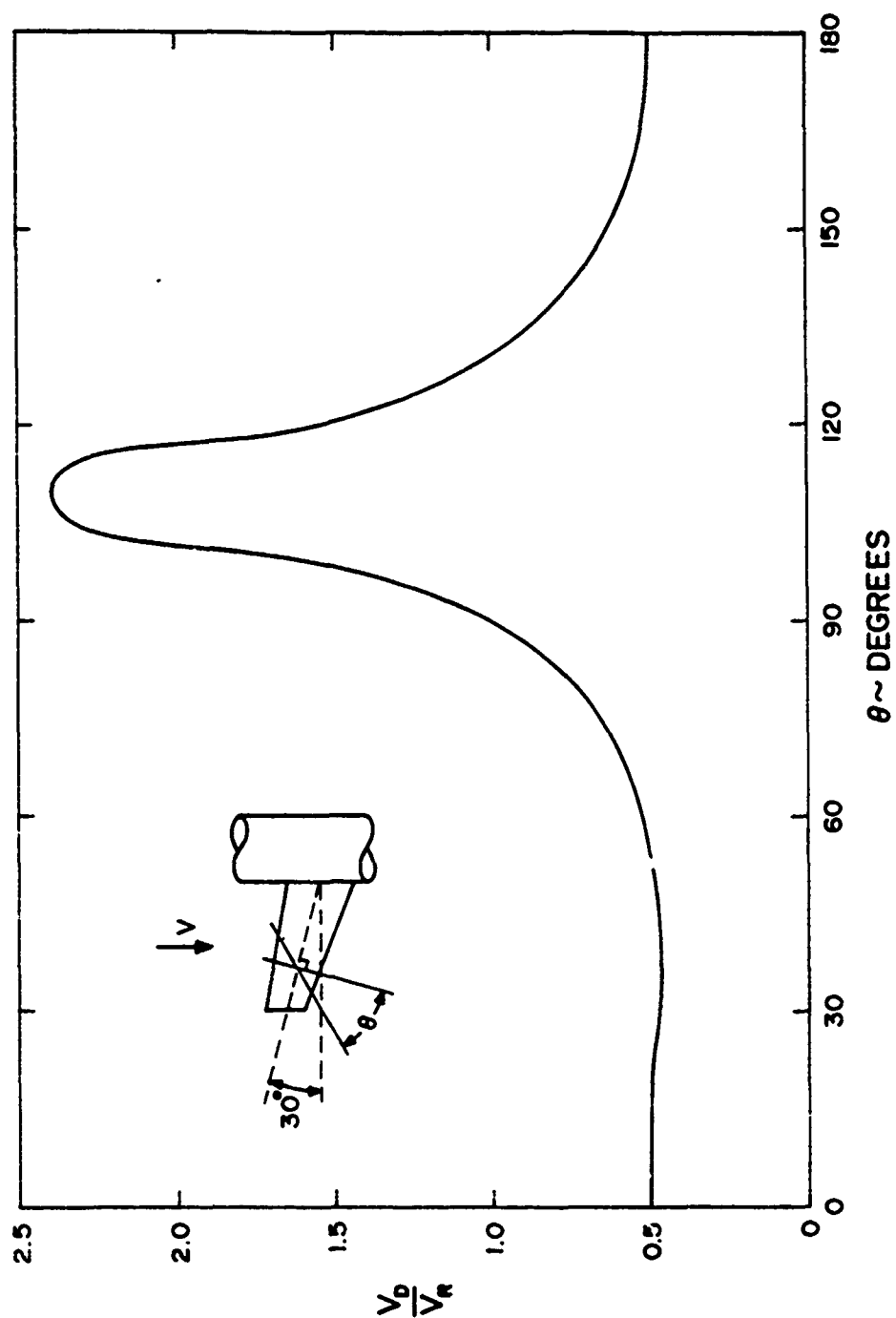


Figure 6- Nondimensional divergence velocity versus fiber orientation for a 30° forward swept wing. Sea level conditions, incompressible fluid. Wing taper ratio is 0.50.

At this position, the wing structure is stiffest from the standpoint of divergence.

To illustrate typical sub-critical aeroelastic characteristics of the laminated, forward swept wing, a situation is examined for which the dynamic pressure is 20% of the divergence dynamic pressure of the wing with θ fibers oriented at 90° . The effect of fiber angle upon aeroelastic stiffness can be seen in Figure 7. In this figure, the parameter $\Delta\bar{y}^*$ is plotted against θ . The parameter $\Delta\bar{y}^*$ represents the spanwise movement (positive outward) of the wing center of lift position, from the center of lift position on the rigid wing, divided by the wing semi-span. Large values of this $\Delta\bar{y}^*$ parameter are associated with large positive changes in the root bending moment. This is true because, for a given flight condition, the lift remains constant. Near the $\theta = 110^\circ$ position, the outward movement of the center of lift is very slight, while, at $\theta = 40^\circ$, a relatively large outward shift in the center of lift can be seen.

Turning to aileron effectiveness, Figure 8 illustrates the behavior of the flexible-to-rigid ratio of $Pb/2V/\delta_0$ versus fiber angle θ for the example wing. Two cases are considered. The first case illustrates the aileron effectiveness of the wing when the ailerons are located between $0.30 \leq 2\bar{y}/b \leq 1.0$, while, in the second case, the ailerons lie in the region $0.30 \leq 2\bar{y}/b \leq 0.80$.

For Case 1, the maximum aileron effectiveness is achieved when $\theta = 125^\circ$, while, for Case 2, maximum effectiveness occurs at $\theta = 115^\circ$. These θ angles are slightly different than the $\theta = 110^\circ$ angle, at which the maximum divergence speed occurs.

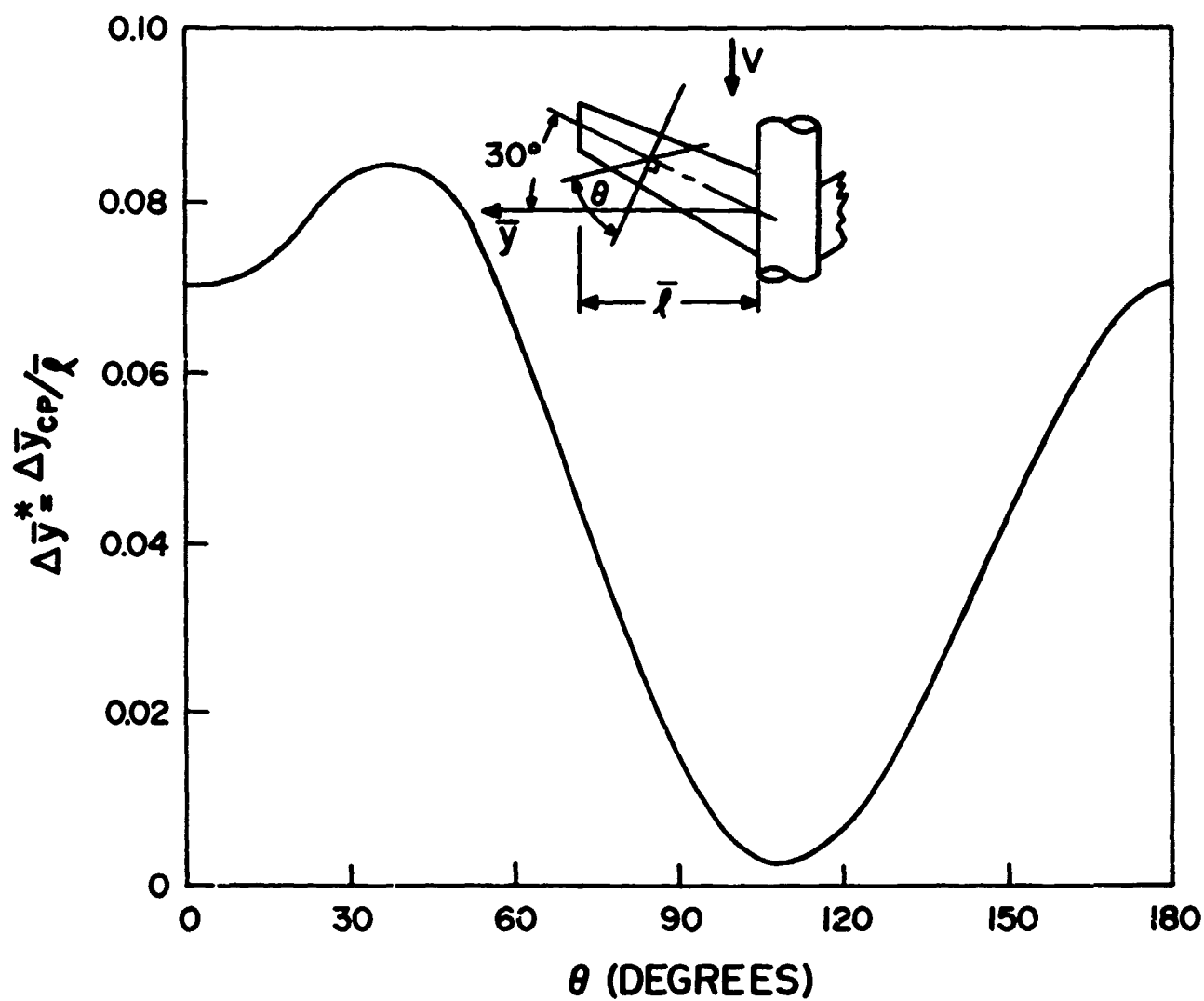


Figure 7- The effect of fiber orientation on the spanwise position of the center of pressure of a wing with 30° of forward sweep. The dynamic pressure is $0.2 q_0$ of the wing when $\theta = 90^\circ$.

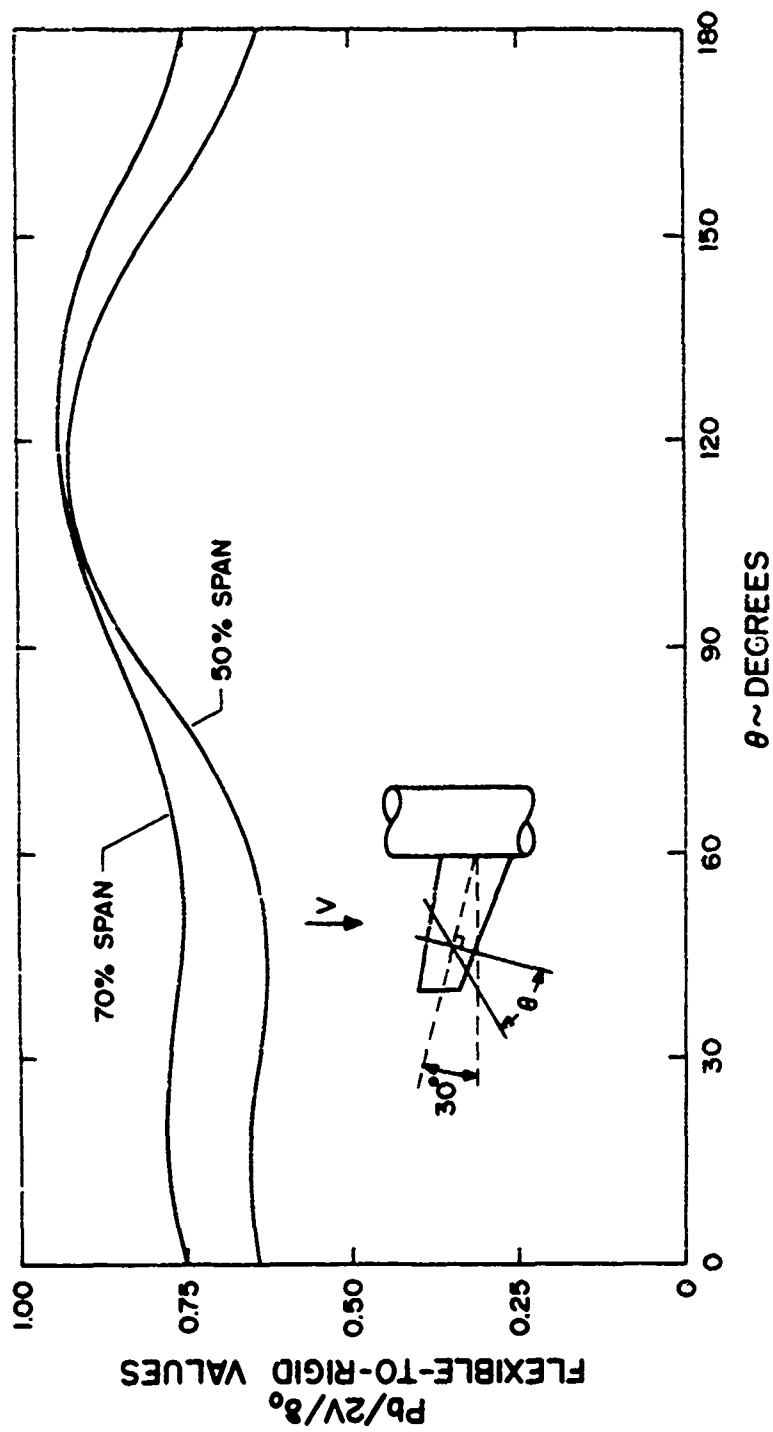


Figure 8- Aileron effectiveness, for a wing with 30° of forward sweep, as a function of θ . Each curve is normalized with respect to the effectiveness of the ailerons on a rigid wing.

SECTION IV

CONCLUSIONS

This report has detailed the results of an investigation of the sub-critical static aeroelastic characteristics of swept wings. In addition, a matrix method of analysis is detailed which will provide an accurate, but low-cost, representation of the aeroelastic behavior of fibrous composite swept wings in subsonic flow. The theories developed have been used in a limited number of cases to illustrate the potential benefits to be gained from aeroelastic tailoring of forward swept wings.

Several important conclusions may be drawn from this analysis:

- (1) The lift coefficient of a flexible wing can be modified greatly by the judicious choice of laminate orientation. Similarly, the wing spanwise center of pressure location can be moved significantly by aeroelastic tailoring.
- (2) The lateral control effectiveness of the wing may be altered by laminate tailoring. However, maximum aileron effectiveness does not occur when the divergence speed is maximized.
- (3) The matrix method developed has the potential for quickly analyzing the effects of laminate construction upon the aeroelastic characteristics of the wing at low cost.

Finally, the techniques developed in this report have been shown to provide an effective means of further exploring the influence of the various parameters upon the static aeroelastic characteristics of laminated, swept wing structures.

APPENDIX A

THE DEVELOPMENT OF THE WING FLEXIBILITY MATRIX

The wing structural idealization used throughout this report consists of a box beam whose flexibility is entirely due to the presence of upper and lower cover-sheets constructed of laminated composite material. This appendix details the development of the flexibility matrix for this type of wing structural model. The laminated beam theory upon which the formulation is based is discussed in detail in Reference 1.

An arbitrary planform wing is shown in Figure A-1 to illustrate the geometry used in the flexibility matrix development. The wing semi-span is divided into a finite number of streamwise panels of arbitrary width h_i . The continuously varying spanwise airload distribution is replaced by a set of discrete running loads, each of which acts upon a streamwise panel and is of constant magnitude over the panel on which it acts.

The loads acting on the wing panels cause wing bending and torsion deformation. The bending and torsion moments caused by the applied loads are computed in local coordinate systems located on each panel as indicated in Figure A-2. This local reference system is swept at an angle Λ_i to the horizontal, with sweepback being positive. The elastic properties of the panel are computed with respect to the local or swept axis.

The development of the flexibility matrix for the composite wing is based upon, and closely parallels, the similar development of a flexibility matrix for a metallic swept wing detailed in Reference 4. The geometry of the structural skeleton of the wing model is shown, for three outboard wing segments, in Figure A-3. Note that this represents the left wing of the

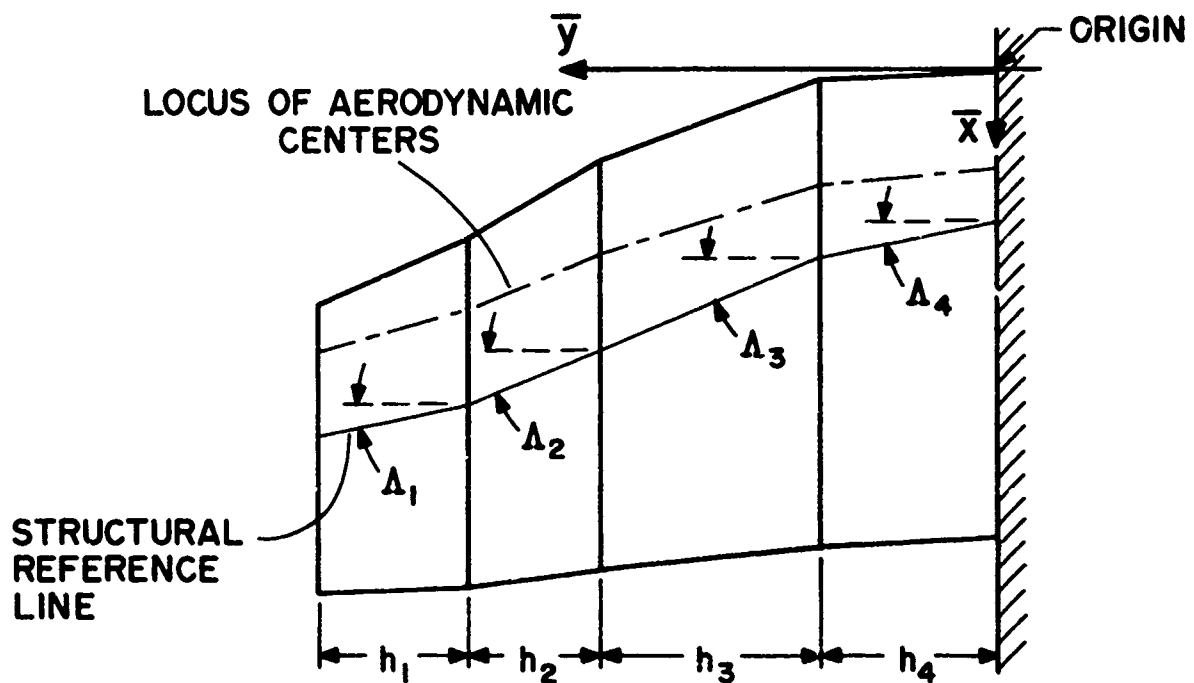


Figure A-1 Four panel wing model showing: spanwise panel dimension h_i ; sweep angle Δ_i ; and segmented aerodynamic centerlines and structural reference axis.

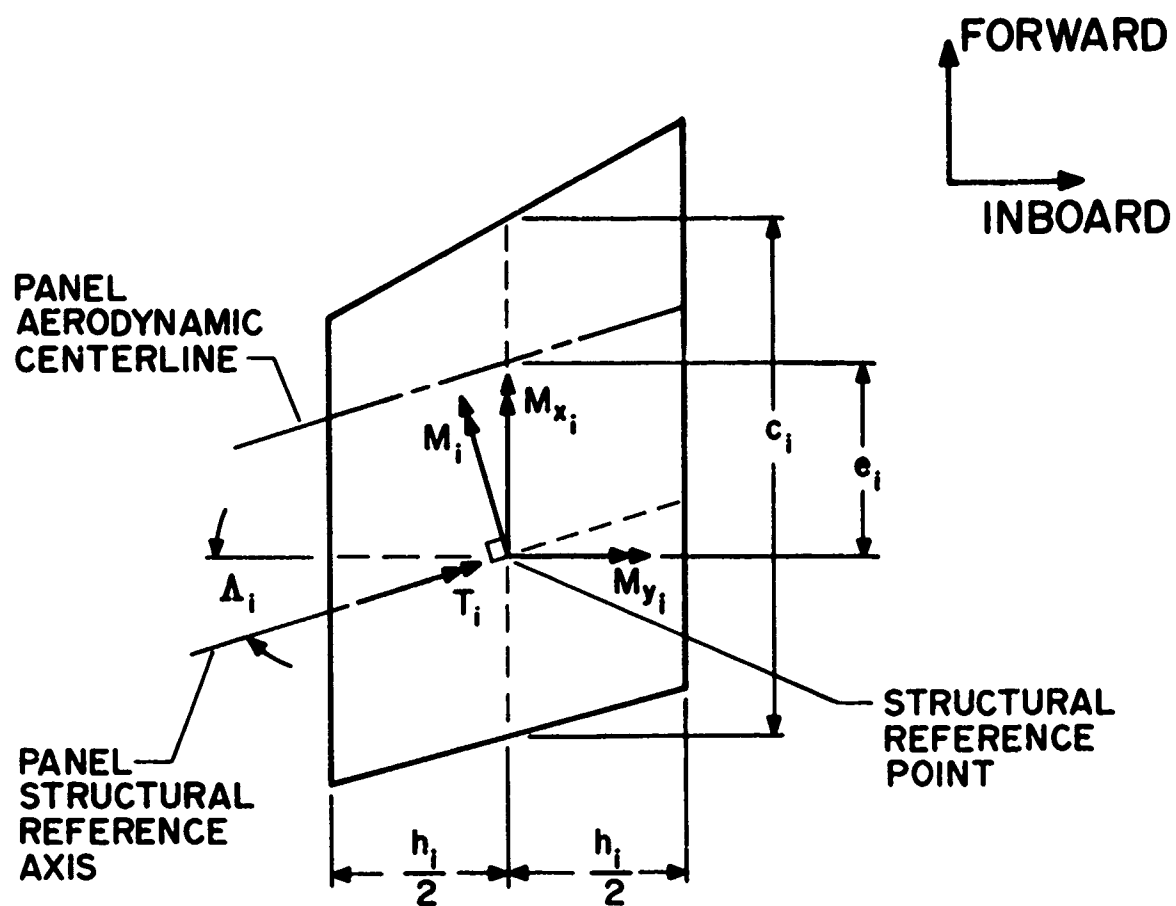


Figure A-2 Typical wing panel geometry with moment sign convention used in derivations.

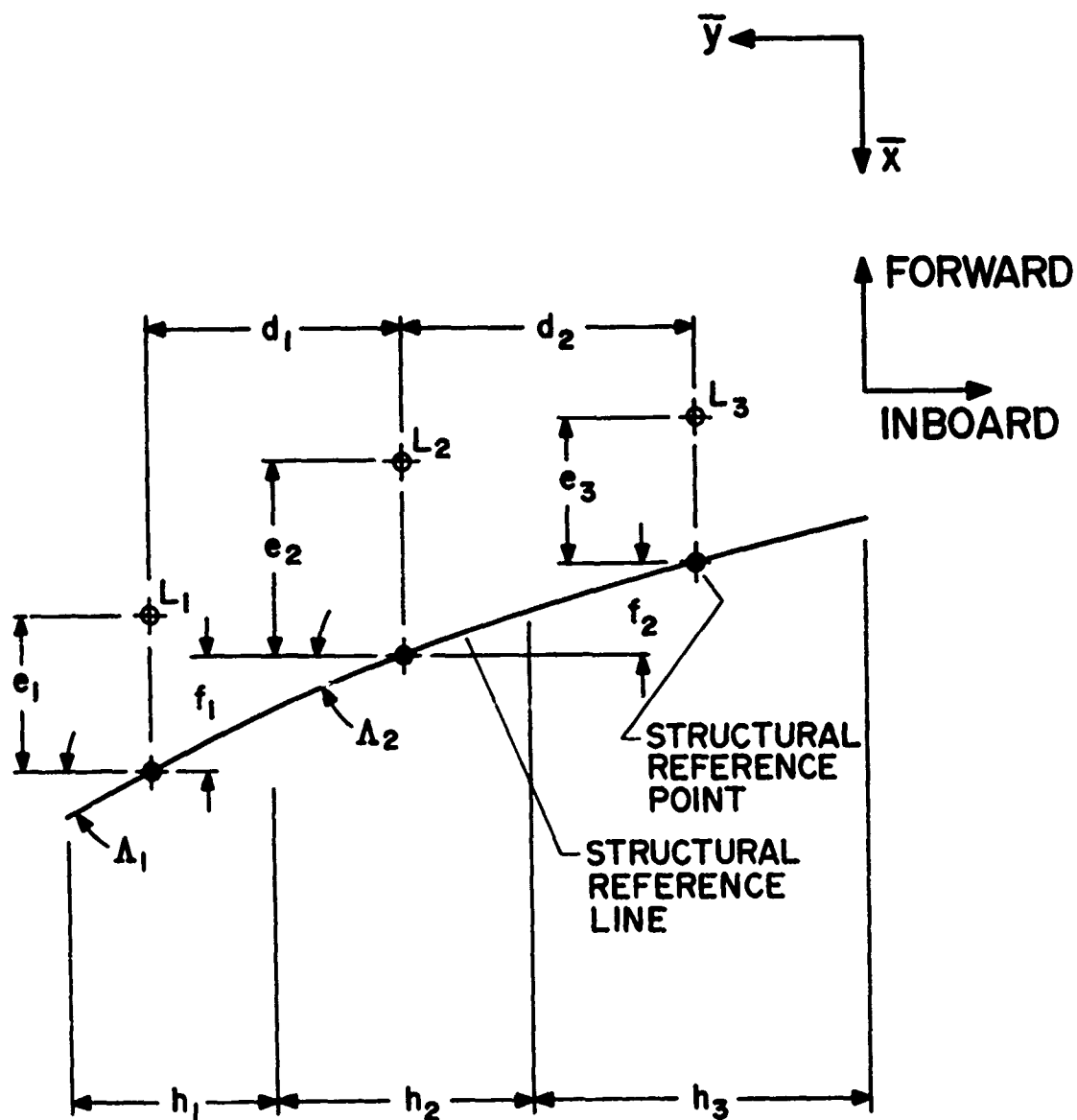


Figure A-3 Plan view of outboard wing sections. Geometrical distances are positive as shown.

aircraft. The definition of the symbols appearing in Figure A-3 is as follows:

- L_i = total lift of a spanwise increment of wing having span h_i . Panel numbering is sequential, beginning with the wing tip.
- e_i = streamwise distance from the aerodynamic center of the panel to the structural reference point, positive when the reference point lies aft of the aerodynamic center.
- f_i = streamwise distance from the structural reference point on a particular panel to the reference point at the next inboard panel. This quantity is positive when the inboard reference point lies forward of the outboard point.
- d_i = lateral distance between the structural reference point of a panel and the structural reference point of the next inboard panel.
- Λ_i = sweep angle of the structural reference axis, positive for sweep-back.
- M_{xi} = rolling moment at a structural reference point due to the lift of all panel segments outboard of this point, positive when it tends to raise the left wing tip. See Figure A-2.
- M_{yi} = pitching moment about the y-axis at a structural reference point, positive nose-up. See Figure A-2.
- M_i = beam bending moment, at a structural reference point, about an axis perpendicular to the local axis, positive when the upper surface is placed in compression.
- T_i = torsional moment, at a structural reference point, about the local axis, positive when it tends to twist the leading edge up.

The structural reference line of the wing is composed of a set of interconnected straight line segments. The reference axis lies midway between the front and the rear edges of the structural box beam. Since the load intensity p_i is assumed constant over each panel, the force acting on each panel at the reference point is

$$L_i = p_i h_i \quad (A-1)$$

where p_i is the running lift per unit spanwise length ($p_i = p_i(y)$). As a result of the lift loads L_i acting on each panel the following bending moments and torques arise [4],

$$\{M\} = \begin{bmatrix} \cos\Lambda & [r_i] & - \sin\Lambda & [u] \end{bmatrix} \{L\} \quad (A-2)$$

$$\{T\} = \begin{bmatrix} \sin\Lambda & [r_2] & + \cos\Lambda & [u] \end{bmatrix} \{L\} \quad (A-3)$$

where

$$\{M\} = \begin{pmatrix} M_1 \\ M_2 \\ M_3 \\ \vdots \\ M_n \end{pmatrix} \quad (A-4)$$

$$\{T\} = \begin{pmatrix} T_1 \\ T_2 \\ T_3 \\ \vdots \\ T_n \end{pmatrix} \quad (A-5)$$

$$\{L\} = \begin{Bmatrix} L_1 \\ L_2 \\ L_3 \\ \vdots \\ L_n \end{Bmatrix} \quad (A-6)$$

$$[\cos \Lambda] = \begin{bmatrix} \cos \Lambda_1 & 0 & 0 & 0 & \cdot & \cdot \\ 0 & \cos \Lambda_2 & 0 & 0 & \cdot & \cdot \\ 0 & 0 & \cos \Lambda_3 & 0 & \cdot & \cdot \\ 0 & 0 & 0 & \cos \Lambda_4 & \cdot & \cdot \\ \cdot & \cdot & \cdot & \cdot & \cdot & \cdot \\ \cdot & \cdot & \cdot & \cdot & \cdot & \cdot \end{bmatrix} \quad (A-7)$$

$$[\sin \Lambda] = \begin{bmatrix} \sin \Lambda_1 & 0 & 0 & 0 & \cdot & \cdot \\ 0 & \sin \Lambda_2 & 0 & 0 & \cdot & \cdot \\ 0 & 0 & \sin \Lambda_3 & 0 & \cdot & \cdot \\ 0 & 0 & 0 & \sin \Lambda_4 & \cdot & \cdot \\ \cdot & \cdot & \cdot & \cdot & \cdot & \cdot \\ \cdot & \cdot & \cdot & \cdot & \cdot & \cdot \end{bmatrix} \quad (A-8)$$

$$[r_2] = \begin{bmatrix} \frac{e_1}{2 \tan \Lambda_1} & 0 & 0 & 0 & 0 & \cdot & \cdot \\ d_1 & \frac{e_2}{2 \tan \Lambda_2} & 0 & 0 & 0 & \cdot & \cdot \\ d_1 + d_2 & d_2 & \frac{e_3}{2 \tan \Lambda_3} & 0 & 0 & \cdot & \cdot \\ d_1 + d_2 + d_3 & d_2 + d_3 & d_3 & \frac{e_4}{2 \tan \Lambda_4} & 0 & \cdot & \cdot \\ d_1 + d_2 + d_3 + d_4 & d_2 + d_3 + d_4 & d_3 + d_4 & d_4 & \frac{e_5}{2 \tan \Lambda_5} & \cdot & \cdot \\ \vdots & \vdots & \vdots & \vdots & \vdots & \vdots & \vdots \end{bmatrix} \quad (A-9)$$

$$[u] = \begin{bmatrix} n & 0 & 0 & 0 & 0 & . \\ e_1 - f_1 & 0 & 0 & 0 & 0 & . \\ e_1 - f_1 - f_2 & 0 & 0 & 0 & 0 & . \\ e_1 - f_1 - f_2 - f_3 & e_2 - f_2 & e_2 - f_2 - f_3 & e_3 - f_3 & 0 & . \\ e_1 - f_1 - f_2 - f_3 - f_4 & e_2 - f_2 - f_3 - f_4 & e_2 - f_2 - f_3 - f_4 & e_3 - f_3 - f_4 & e_4 - f_4 & . \\ . & . & . & . & . & . \\ . & . & . & . & . & . \end{bmatrix} \quad (A^{-1}(0))$$

$$[r_1] = \begin{bmatrix} \frac{h_1}{4 \cos^2 \Lambda_1} - \frac{e_1 \tan \Lambda_1}{2} & 0 & 0 & 0 & 0 \\ d_1 & \frac{h_2}{4 \cos^2 \Lambda_2} - \frac{e_2 \tan \Lambda_2}{2} & 0 & 0 & 0 \\ d_1 + d_2 & d_2 & \frac{h_2}{4 \cos^2 \Lambda_3} - \frac{e_3 \tan \Lambda_3}{2} & 0 & 0 \\ d_1 + d_2 + d_3 & d_2 + d_3 & d_3 & \frac{h_4}{4 \cos^2 \Lambda_4} - \frac{e_4 \tan \Lambda_4}{2} & 0 \\ d_1 + d_2 + d_3 + d_4 & d_2 + d_3 + d_4 & d_3 + d_4 & d_4 & \frac{h_5}{4 \cos^2 \Lambda_5} - \frac{e_5 \tan \Lambda_5}{2} \end{bmatrix} \quad (A-11)$$

The objective of the flexibility matrix development is to define a relationship between the load intensities p_i on each wing panel and the streamwise angle of attack on each panel, α_i . This development is accomplished through the energy methods and the use of the dummy unit load method. For the linear elastic laminated beam model discussed in Reference 1, the present study has determined that the strain energy, expressed in terms of the bending moment M and twisting moment T , is

$$U = \frac{1}{2} \int_0^l \frac{1}{1 - kg} \left\{ \frac{M^2}{EI} + \frac{2MTK}{EI GJ} + \frac{T^2}{GJ} \right\} ds \quad (A-12)$$

where EI , GJ and K are the bending stiffness, torsional stiffness and coupling parameter values, respectively for the beam and

$$k = K/EI \quad g = K/GJ \quad (A-13a,b)$$

$$ds = \text{incremental distance along the reference axis} \quad (A-13c)$$

Note that all values are computed with respect to the structural reference axis. The streamwise angle of attack distribution, $\alpha(s)$, along the wing, resulting from the bending moment and twisting moment distributions, may be found by using Castigliano's Theorem to derive the following relationship for α .

$$\alpha = \int_0^l \frac{1}{(1 - kg)} \left(\frac{Mm}{EI} + \frac{g(Mt + Tm)}{EI} + \frac{Tt}{GJ} \right) ds \quad (A-14)$$

The terms m and t in Equation (A-14) are, by definition, the bending moment and twisting moment, respectively, that arise when a unit pitching moment (positive nose-up) is applied at a position on the wing where α is to be computed. Note that the unit pitching moment is applied perpendicular to the free stream while m and t are computed along the reference axis. Equation

(A-14) may be used to compute α in matrix form. The vector $\{\alpha\}$ represents the set of streamwise angles of attack computed at the spanwise midpoint of each wing panel. The values of EI, GJ and K are taken to be constant for each panel and are those values computed at the panel reference point.

The general procedure for deriving the flexibility matrix for an isotropic metallic wing is detailed in Reference 4. Following the same procedure for the laminated beam model, the flexibility matrix $[C_{ij}]$ is defined such that the lift distribution $\{p_j\}$ is related to $\{\alpha_i\}$.

$$\{\alpha_i\} = [C_{ij}] \{p_j\} \quad (A-15)$$

The expression for $[C_{ij}]$ reads:

$$\begin{aligned} [C_{ij}] = [I_0] & \begin{bmatrix} 0 & 0 \\ \frac{h(g - \tan\Lambda)}{EI(1 - kg)} & 0 \end{bmatrix} \begin{bmatrix} 0 & 0 \\ [\cos\Lambda][r_1] - [\sin\Lambda][u] \end{bmatrix} \begin{bmatrix} 0 \\ [h] \end{bmatrix} \\ & + [I_0] \begin{bmatrix} 0 & 0 \\ \frac{h(1 - k\tan\Lambda)}{GJ(1 - kg)} & 0 \end{bmatrix} \begin{bmatrix} 0 & 0 \\ [\sin\Lambda][r_2] + [\cos\Lambda][u] \end{bmatrix} \begin{bmatrix} 0 \\ [h] \end{bmatrix} \end{aligned} \quad (A-16)$$

where

$$[I_0] = \begin{bmatrix} \frac{1}{2} & 1 & 1 & 1 & . & . \\ 0 & \frac{1}{2} & 1 & 1 & . & . \\ 0 & 0 & \frac{1}{2} & 1 & . & . \\ 0 & 0 & 0 & \frac{1}{2} & . & . \\ . & . & . & . & . & 0 \\ . & . & . & . & . & . \end{bmatrix} \quad (A-17)$$

In Equation (A-16), note the $[\begin{smallmatrix} 0 \\ 0 \end{smallmatrix}]$ refers to a diagonal matrix. If k and g are zero, the expression given in Equation (A-16) reduces to that derived in Reference 4.

APPENDIX B

THE AERODYNAMIC INFLUENCE COEFFICIENT MATRIX

This appendix reviews the theoretical development of the aerodynamic influence coefficient matrix $[A_{ij}]$ used in this study. The development is taken from, and is identical to, that developed in Reference 4.

The spanwise lift distribution on an aircraft wing varies in the lateral direction and may be visualized as resulting from a system of horseshoe vortices, each of constant strength, Γ_i , placed along the wing as indicated in Figure B-1. The double arrows indicate that the sense of the circulation around each vortex line segment is given by the right hand rule.

With the type of aerodynamic model shown above, the net strength of the trailing vortex at any point on the wing span is numerically equal to the rate of change of strength of the bound vortex in the spanwise direction. The degree of accuracy required in the analysis and the wing planform shape determines the number and position of these horseshoe vortices.

For a given wing planform geometry, the spanwise lift distribution is determined by the local streamwise angle of attack distribution and the sectional 2-D lift-curve-slope distribution. The unknowns in the problem are the values of running lift, p_i , at points along the wing span. To compute the relationship between the local angles of attack, at points along the wing expressed as the vector $\{\alpha_i\}$, and the values of running lift at these same points, given as the vector $\{p_i\}$, the following linear relationship is used.

$$\{\alpha_i\} = [A_{ij}] \{p_j\} \quad (B-1)$$

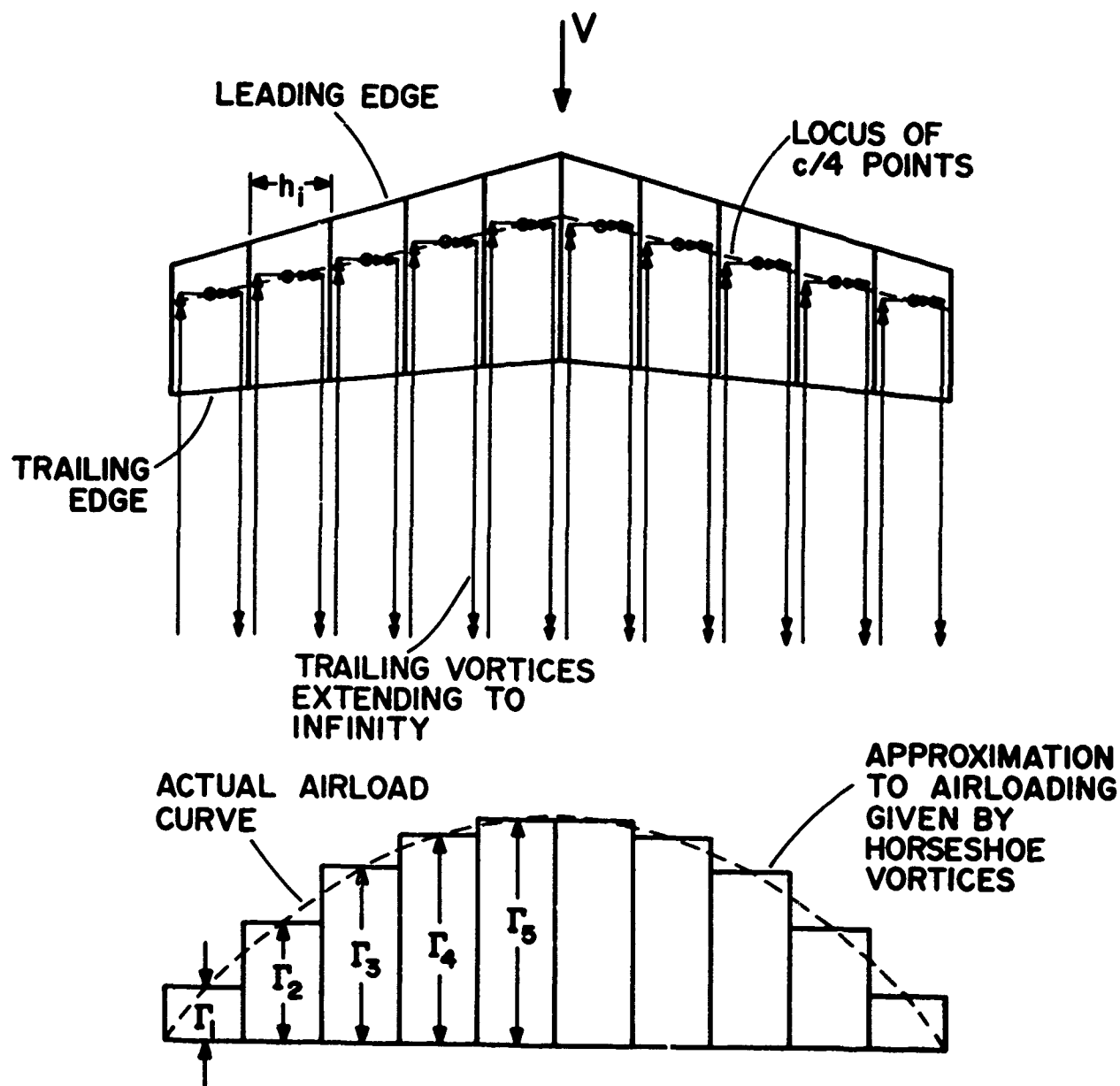


Figure B-1 Horseshoe vortex system used to approximate the actual airload distribution on the wing.

where $[A_{ij}]$ is referred to as the aerodynamic influence coefficient (AIC) matrix.

To compute the elements A_{ij} , we begin by subdividing the wing into a series of panels of spanwise width h_i , as shown in Figure B-1. In this figure, the horseshoe vortices are bound to a point at the wing panel quarter-chord line intersection with the panel midspan.

For a symmetrical planform at zero yaw angle, it is always possible to treat any spanwise airload distribution as the sum of two airload distributions, one which is symmetrical with respect to the planform centerline and the other which is antisymmetrical with respect to the planform centerline. This feature considerably simplifies computation of the A_{ij} elements since the specification that the lift distribution is either symmetrical or antisymmetrical allows the AIC computations to be restricted to one-half of the total wing. This wing half is taken to be the left wing of the aircraft.

The AIC matrix is given by the following expression

$$[A_{ij}] = \left[\frac{1}{4a_0} \right] [S_{ij}] \quad (B-2)$$

where

a_0 = 2-D lift-curve-slope at wing position (i).

The elements of $[S_{ij}]$ are defined in terms of the geometrical position of the panel quarter-chord points. These expressions are somewhat lengthy and are not reproduced here. The reader is referred to Reference 4 for a detailed discussion of the derivation of the AIC's.

APPENDIX C

TWIST CAUSED BY CONTROL DEFLECTION PITCHING MOMENT

The deflection of a control surface on a wing results in two effects that change the local angle of attack of the wing. The first of these effects is an apparent angle of attack due to control deflection, written as

$$\alpha = \frac{\partial \alpha}{\partial \delta} \delta \quad (C-1)$$

where δ is the control surface deflection. The second effect of the deflection of a control surface is a twisting of the wing caused by a change in the pitching moment due to control deflection. It is to this latter effect that attention is now turned.

When an aileron is deflected, a streamwise pitching moment results. This pitching moment T_y is given by

$$T_y = (qc^2 c_{m\delta}) \delta \quad (C-2)$$

On a flexible wing, this pitching moment will cause deformation that, in turn, will lead to changes in the spanwise lift distribution. The computation of this lift distribution is necessary to the determination of the roll control effectiveness of an aircraft.

As part of the present study, the matrix relating control surface deflection to the streamwise angle of attack was determined for a laminated composite beam model. For this model, the bending moment and twisting moment vectors, computed at the structural reference points of the left hand wing panels are given as [4]

$$\{M\}_\delta = -q[\sin\Lambda][I_0]^T[hc^2 c_{m\delta}]\{\delta\} \quad (C-3)$$

$$\{T\}_\delta = q[\cos\Lambda][I_0]^T[hc^2 c_{m\delta}]\{\delta\} \quad (C-4)$$

Utilizing the unit load method, together with laminated beam theory, the angle of attack distribution $\{\alpha_\delta\}$ caused by the pitching moment given in Equation (C-2) is given by the expression

$$\begin{aligned} \{\alpha_\delta\} = [m] & \left\{ \left[\frac{h}{EI(1 - kg) \cos \Lambda} \right] \{M\} + \left[\frac{gh}{EI(1 - kg) \cos \Lambda} \right] \{T\} \right. \\ & \left. + [t] \left\{ \left[\frac{h}{GJ(1 - kg) \cos \Lambda} \right] \{T\} + \left[\frac{kh}{GJ(1 - kg) \cos \Lambda} \right] \{M\} \right\} \right\} \quad (C-5) \end{aligned}$$

$$\text{where} \quad [m] = -[I_o] \sin \Lambda \quad (C-6)$$

$$\text{and} \quad [t] = [I_o] \cos \Lambda \quad (C-7)$$

The matrix $[I_o]$ is defined in Equation (A-17).

Combining Equations (C-3) and (C-4) with Equation (C-5) yields a relationship of the form

$$\{\alpha_\delta\} = q[E_{ij}] \{\delta\} \quad (C-8)$$

where

$$\begin{aligned} [E_{ij}] = [I_o] & \left[\frac{h(\sin \Lambda)(\tan \Lambda - g)}{EI(1 - kg)} \right] [I_o]^T [hc^2 c_{m\delta}] \\ & + [I_o] \left[\frac{h(\cos \Lambda)(1 - k \tan \Lambda)}{GJ(1 - kg)} \right] [I_o]^T [hc^2 c_{m\delta}] \quad (C-9) \end{aligned}$$

The matrix defined in Equation (C-9) reduces to that defined in Reference 4 (p. 88) for a metallic wing.

APPENDIX D
THE STIFFNESS EXPRESSIONS FOR A
LAMINATED COMPOSITE BOX BEAM

The wing structural model employed throughout this report is described in detail in Reference 1 and is based upon the assumption that the bending stiffness and torsional stiffness of the wing structure are due entirely to the presence of relatively thin, laminated composite cover sheets. Although all of the bending and torsional stiffness is assumed to reside entirely in the laminated cover sheets, it would be a simple task to add algebraically any additional stiffnesses that might arise from the presence of such elements as spar caps or flexible webs.

To formulate the expression for the equivalent bending stiffness, EI , and torsional stiffness, GJ , for this type of box-beam structure, it is necessary to make an assumption about the deformation behavior of the wing box. The well-known Euler-Bernoulli hypothesis that the strain due to bending varies linearly from the neutral surface of the box-beam provides this assumption about the displacement behavior of the wing. In addition, it is further hypothesized that chordwise sections of the wing, perpendicular to a beam reference axis, are rigid. This means that the deformation of the wing box is a function only of a spanwise coordinate, y . The material behavior is assumed to be linear elastic. An additional feature of the idealized beam model is that the reference surface of the box beam is taken at the geometrical middle surface of the wing box. This convention, commonly used in laminated plate theory, is more convenient than the alternative of locating a modulus weighted centroid of each beam cross-section

(a modulus weighted centroidal axis will always lie in the neutral surface). If the laminated box beam is not both elastically and geometrically symmetrical, the middle surface will not be the neutral surface for bending.

A Cartesian coordinate system is defined in Figure D-1. The x-y plane corresponds to the geometrical middle surface of the wing box. The positive x-axis is rearward on the wing while the y-axis lies along the swept wing span and is coincident with the chordwise centerline of the wing box.

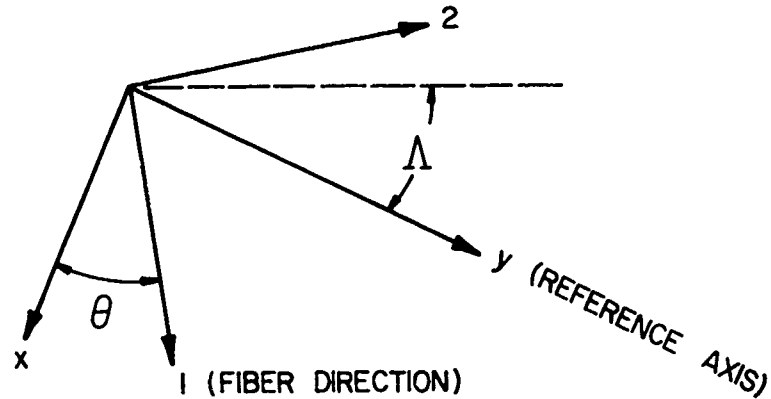


Figure D-1 - Composite material lamina principal axes, 1 and 2, with respect to the wing reference axes, x and y.

For a single orthotropic lamina, the relationship between membrane stresses and strains occurring in the beam laminae can be written, in matrix notation, as:

$$\begin{Bmatrix} \sigma_{yy} \\ \tau_{xy} \end{Bmatrix} = \begin{bmatrix} \bar{Q}_{22} & \bar{Q}_{26} \\ \bar{Q}_{26} & \bar{Q}_{66} \end{bmatrix} \begin{Bmatrix} \epsilon_{yy} \\ \gamma_{xy} \end{Bmatrix} \quad (D-1)$$

The terms \bar{Q}_{ij} are functions of the orthotropic engineering constants, Q_{ij} , and the angle θ defining the orientation between the lamina principal axes and the box-beam reference axes [5]. The lamina lies in a plane

parallel to the x-y plane; the angle θ is as defined in Figure D-1.

The constitutive relations for the inplane or membrane behavior of the individual lamina are used to determine the strain energy functional for the box beam. In this case, the individual laminae are constrained to act as a unit because of the Euler-Bernoulli assumption. From this strain energy functional, the equilibrium equations for the wing may be derived.

The governing equations of equilibrium contain the expressions for the equivalent EI, GJ and K, the bending-torsion coupling parameter. These terms are

$$EI = EI_0 - \frac{(B_{22})^2}{A_{22}} \quad (D-2)$$

$$GJ = GJ_0 - \frac{(B_{33})^2}{A_{22}} \quad (D-3)$$

$$K = K_0 - \frac{B_{22}B_{33}}{A_{22}} \quad (D-4)$$

where

$$EI_0 = b \left[\sum_{i=1}^N \bar{Q}_{22}^{(i)} \beta_i \right] \quad (D-5)$$

$$GJ_0 = b \left[\sum_{i=1}^N 4\bar{Q}_{66}^{(i)} \beta_i \right] \quad (D-6)$$

$$K_0 = b \left[\sum_{i=1}^N 2\bar{Q}_{26}^{(i)} \beta_i \right] \quad (D-7)$$

$$A_{22} = b \left[\sum_{i=1}^N \bar{Q}_{22}^{(i)} t_i \right] \quad (D-8)$$

$$B_{22} = b \left[\sum_{i=1}^N \bar{Q}_{22}^{(i)} \delta_i \right] \quad (D-9)$$

$$B_{33} = 2b \left[\sum_{i=1}^N \bar{Q}_{26}^{(i)} \delta_i \right] \quad (D-10)$$

and b represents the chordwise width of the box beam. The summation in the equations extends over the N layers of composite material. The constants β_i and δ_i are defined in terms of lamina coordinates with respect to the middle surface. In terms of the lamina thickness t_i and lamina lower and upper position coordinates z_i and z_{i+1} , respectively, β_i and δ_i are defined as follows

$$\begin{aligned} \beta_i &= \int_{z_i}^{z_{i+1}} z^2 dz \\ &= \frac{1}{3} (t_i^3 + 3t_i z_i^2 + 3z_i t_i^2) \end{aligned} \quad (D-11)$$

and

$$\begin{aligned} \delta_i &= \int_{t_i} z dz \\ &= t_i (z_{i+1} + z_i) / 2 \end{aligned} \quad (D-12)$$

The term β_i represents the area moment of inertia of a strip of material, of thickness t_i and unit width, about the middle surface. As such, β_i is always a positive number. The term δ_i represents the first moment of the

area of the same strip about the middle surface. This term δ_i is positive if the lamina area centroid lies above the middle surface and negative if it does not.

REFERENCES

1. T. A. Weisshaar, "Aeroelastic Stability and Performance Characteristics of Aircraft with Advanced Composite Sweptforward Wing Structures", AFFDL-TR-78-116, September 1978.
2. F. W. Diederich and K. A. Foss, "Charts and Approximate Formulas for the Estimation of Aeroelastic Effects on the Loading of Swept and Unswept Wings", NACA TN 2608, September 1951.
3. R. L. Bisplinghoff, H. Ashley and R. L. Halfman, Aeroelasticity, Addison-Wesley, pp. 474-479, 1955.
4. W. L. Gray and K. L. Schenk, "A Method for Calculating the Subsonic Steady-State Loading on an Airplane with a Wing of Arbitrary Plan Form and Stiffness", NACA TN 3030, July 1953.
5. R. M. Jones, Mechanics of Composite Materials, McGraw-Hill, pp. 47-59, 1975.